Supporting Information

For paper entitled: A Mechanistic Model of the Intravitreal Pharmacokinetics of Large Molecules and the Pharmacodynamic Suppression of Ocular VEGF Levels by Ranibizumab in Patients with Neovascular Age-related Macular Degeneration.

Authors: Laurence A. Hutton-Smith, Eamonn A. Gaffney, Helen M. Byrne, Philip K. Maini, Dietmar Schwab and Norman A. Mazer.

S1. Approximation for S_*/S

Here we estimate the ratio S_*/S for the human, monkey and rabbit based on the anatomically accurate models of the eye given by Missel[1].

Figure S1.1 Ocular anatomical regions of interest for the human, monkey and rabbit, based on Figure 4 of Missel PJ (Simulating Intravitreal Injections in Anatomically Accurate Models for Rabbit, Monkey, and Human Eyes. *Pharm. Res.* 2012, *29* (12), 3251–3272.) Line segments denote lengths that are used to calculate the surface area S_* corresponding to the vitreous/ aqueous interface for each species including the space of Petit.

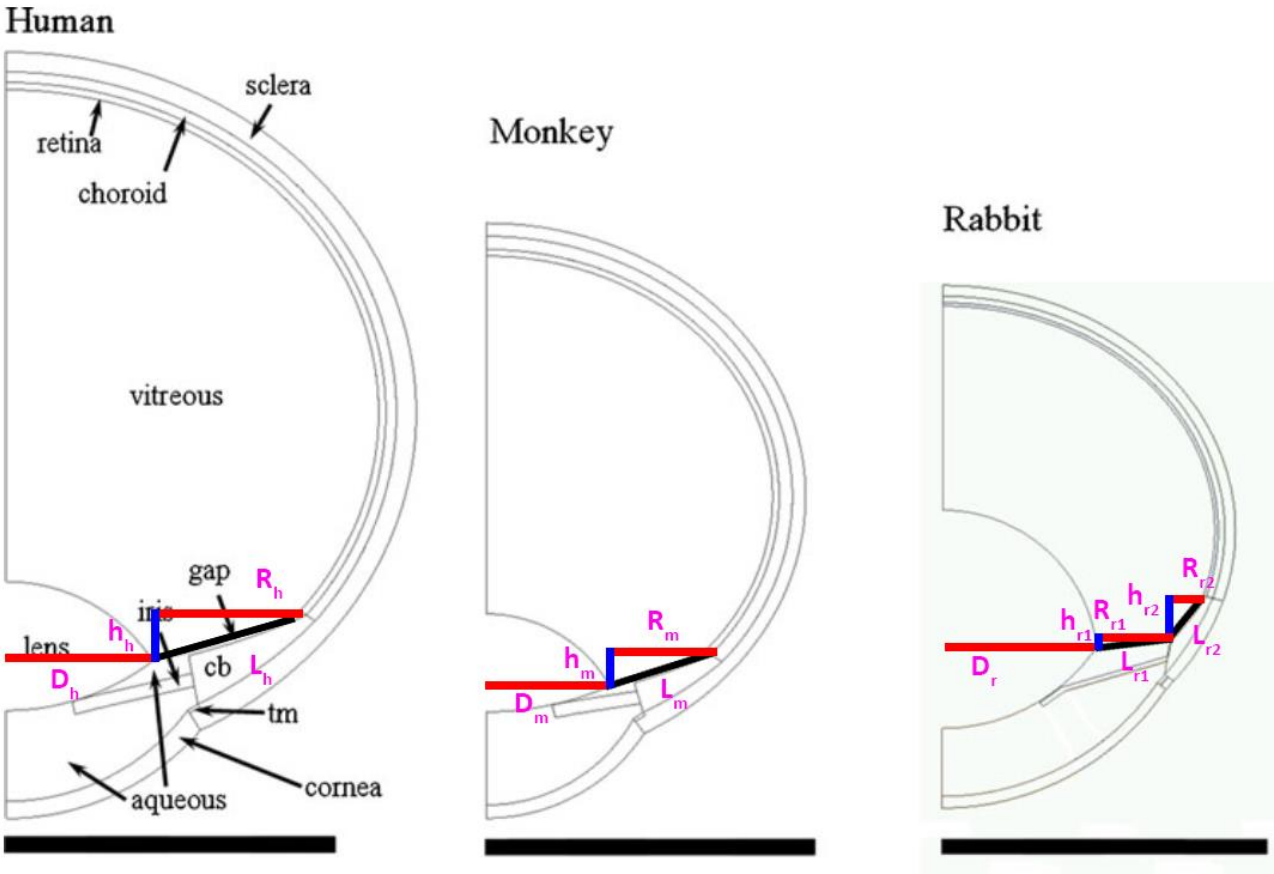

Table S1.2 Geometric quantities of anatomical regions

Species	Region	Length (cm) (or cm^2 for surface area)
Human	R_h	0.4516
	D_h	0.4506
	h_h	0.1498
	S_h	13.18 (cm^2)
Monkey	R_m	0.3058
	D_m	0.3578
	h_m	0.1030
	S_m	8.11 (cm^2)
Rabbit	R_{r1}	0.2202
	R_{r2}	0.1050
	D_r	0.4444
	h_{r1}	0.0173
	h_{r2}	0.1213
	S_r	6.39 (cm^2)

Note: S is the total surface area of vitreous chamber calculated from r_{vit} (given in Table 4)

The formula for the surface revolution (for L) of conical frustum used to calculate S_*.

$$A_L = \pi(R_1 + R_2)\sqrt{(R_1 - R_2)^2 + h^2}$$

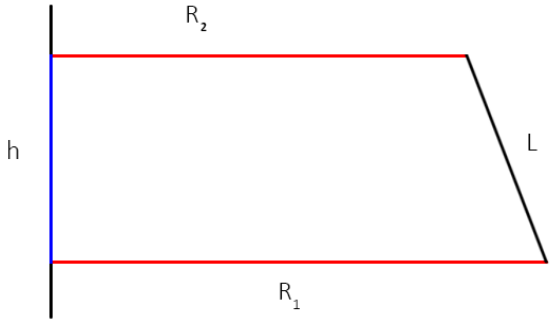

Species	**Region interpreted as S_***	**S_* (cm^2)**
Human	L_h	2.0219
Monkey	L_m	1.0354
Rabbit	L_{r1}+ L_{r2}	1.4924

Species	**S_*/S**
Human	0.15
Monkey	0.13
Rabbit	0.23
Mean	**0.17**

S2. Estimates of the ocular $t_{1/2}$ and T_{diff} for bevacizumab in the rat

Chuang et al. reported bevacizumab serum concentrations following the intravitreal injection of 0.125 mg bevacizumab to Sprague-Dawley rats (250 to 350 g in body weight)[2]. Data from control animals (who did not undergo experimental retinal vein occlusion) are shown in Figure S2. The IVT PK model used fit to this data was obtained by convoluting the ocular input function, I(t), defined as:

Eq. S2.1 $$I(t) = F\ d\ \exp[-\ln(2)/(t_{1/2})\ (t - t_{lag})]$$

with the 2-compartment IVT PK model derived by Lin et al. for the intravenous administration of 0.66 mg/kg to Sprague-Dawley rats[3], which we parameterize as:

Eq. S2.2 $$C(t) = 1/V\ [(\alpha - k_{21})/(\alpha - \beta)]\ \exp(-\alpha t) + [(k_{21} - \beta)/(\alpha - \beta)]\ \exp(-\beta t)$$

For the input function, F is the bioavailability of the IVT route, d is the IVT dose (taken as 0.4167 mg/kg), $t_{1/2}$ is the ocular half-life and T_{lag} is the absorption lag time. For the 2-compartment model the parameters values were derived from the values reported by Lin et al.:

$$\alpha = 2.221\ day^{-1},\ \beta = 0.128\ day^{-1},\ k_{21} = 0.803\ day^{-1} \text{ and } V = 25\ mL/kg$$

The input function parameters were estimated by a least squares fit of the model to the Chuang data (using the Excel solver) and corresponded to: F = 0.555, $t_{1/2}$ = 0.341 day and T_{lag} = 0.19 day with an RMSE in the fit of 84.3 ug/mL.

Figure S2: Mean serum concentrations of bevacizumab following IVT administration to Sprague-Dawley rats (from Chuang et al). Dashed curve is fit to an IVT PK model based on the convolution of an ocular input function and 2-compartment model (Equations S2.1 and S2.2). The estimated value of the ocular $t_{1/2}$ is 0.341 days.

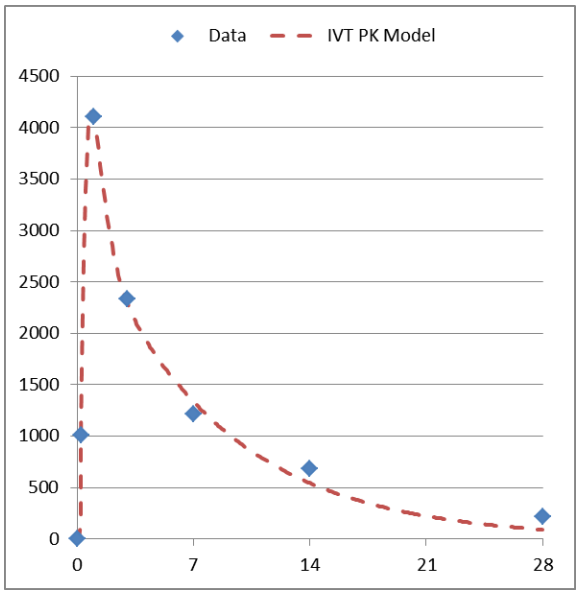

The value of F was similar to that reported for ranibizumab in the monkey[4]. The fit of the model to the peak serum concentration was sensitive to the value of $t_{1/2}$. The estimated value of 0.341 days in the rat is notably smaller than the $t_{1/2}$ values for IgG observed in the rabbit and monkey[5,6] (see Table 4 of main text).

The value of T_{diff} in the rat was estimated from Equation (1) to be 0.10 days, where r_{vit} was calculated from the vitreous volume Vol_{vit} of 42 µL for 70 day-old Sprague-Dawley rats weighing 300 g[7,8].

S3. Individual patient plots of VEGF profiles and model fit for K_D = 21,000 pM

Each figure shows the experimental data and optimized model fit to an individual subject corresponding to a K_D value of 21,000 pM. The estimated values of $t_{1/2}$ and P_{in} are given in the legend. Patient numbers are those used by Sanders et al.[9]

Figure S3.1

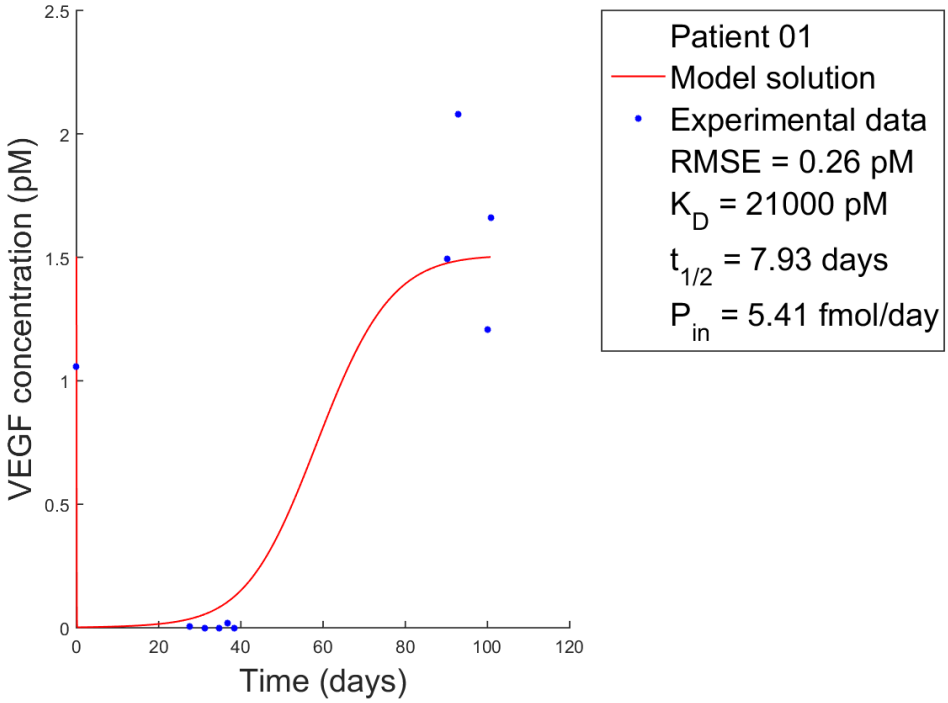

Figure S3.2

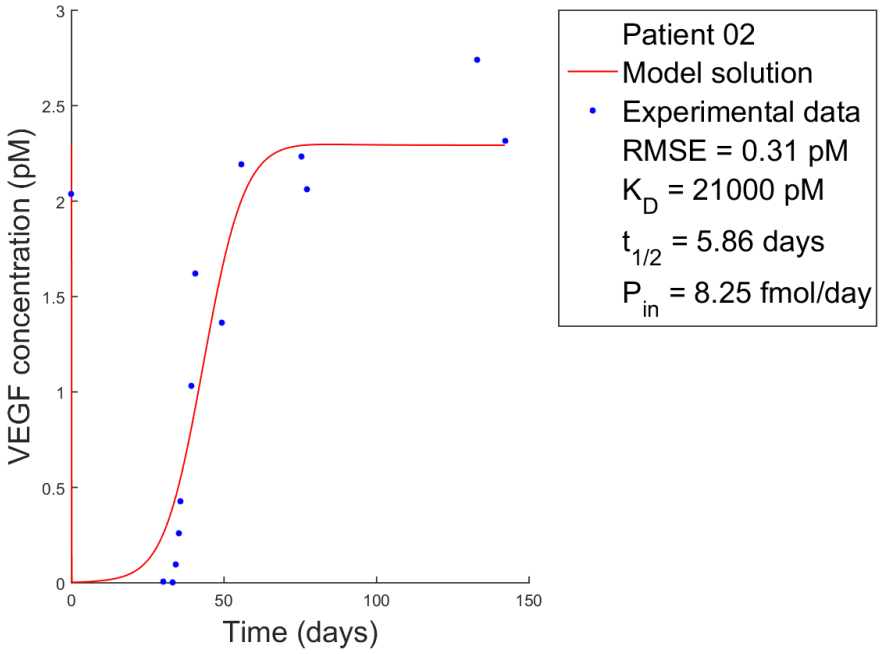

Figure S3.3

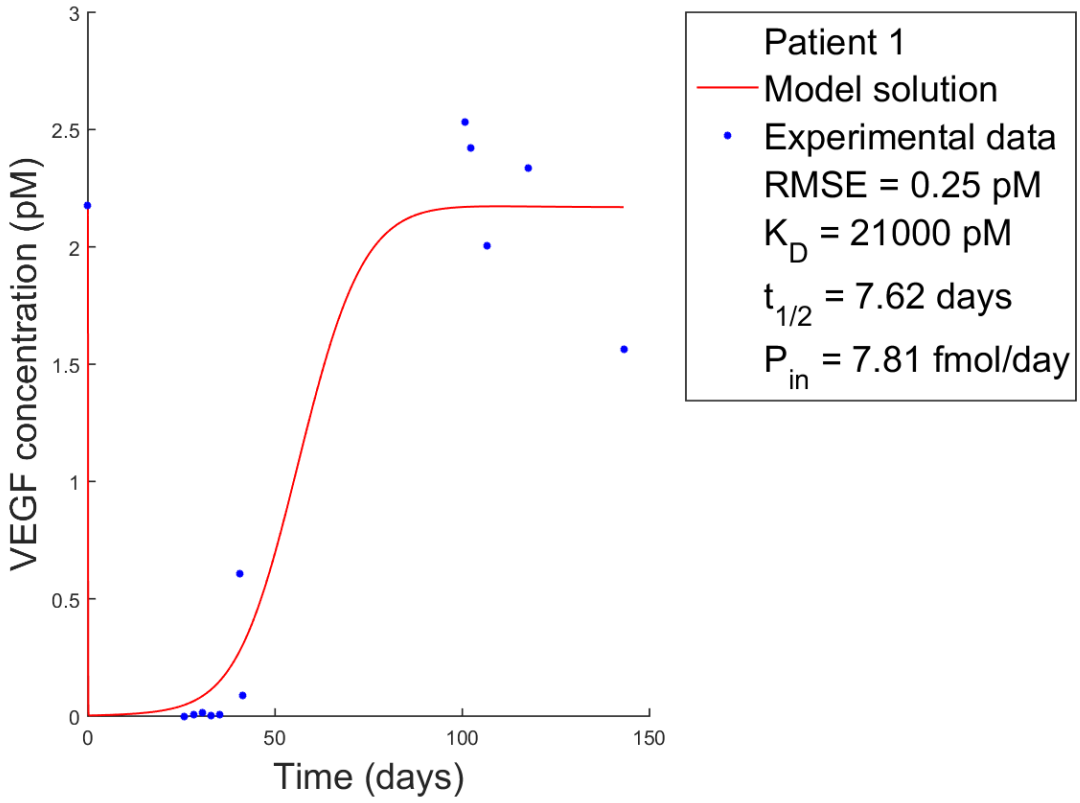

Figure S3.4

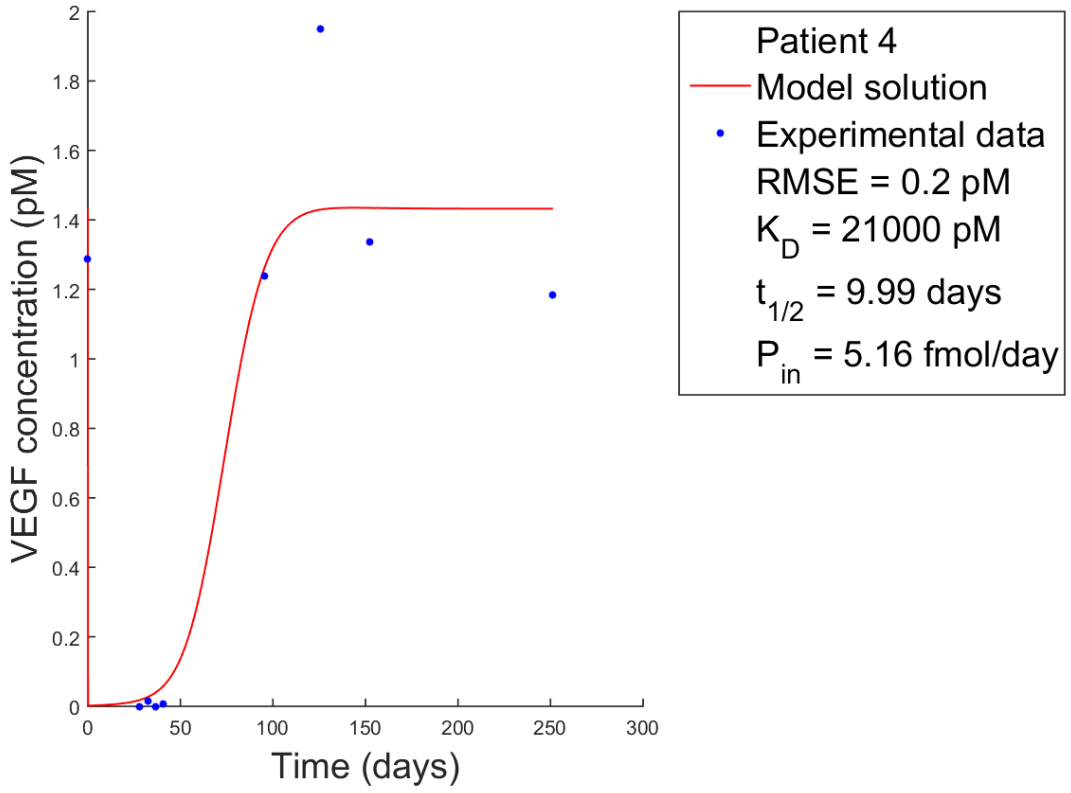

Figure S3.5

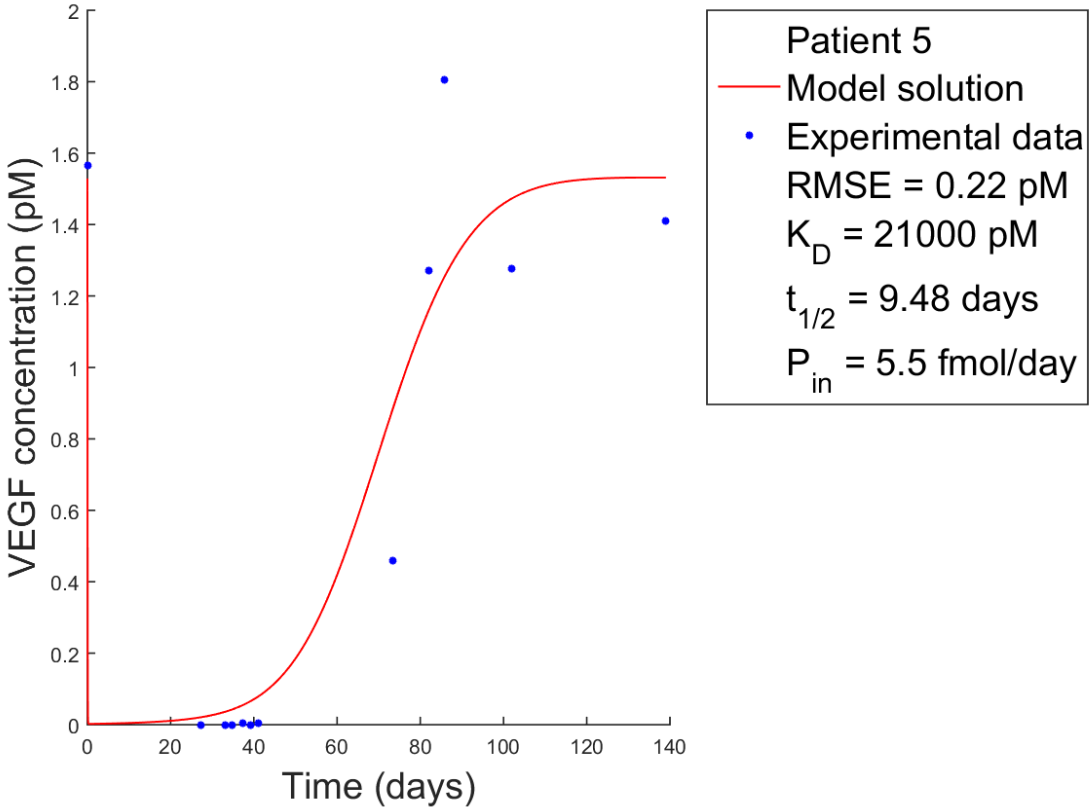

Figure S3.6

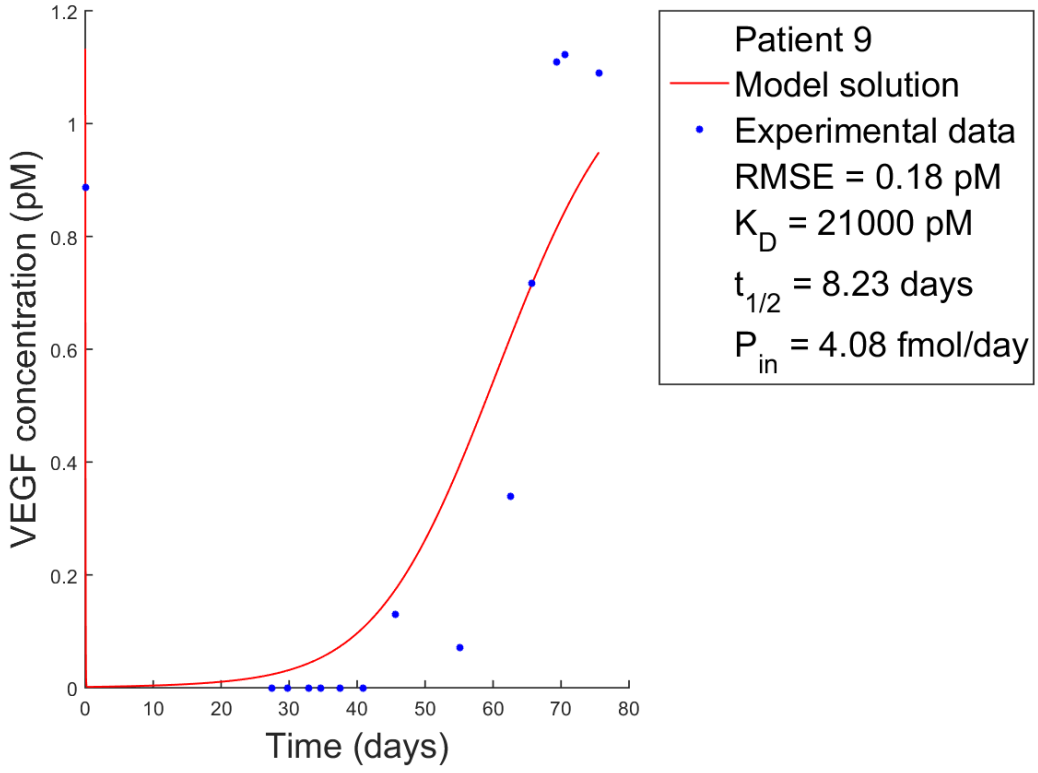

Figure S3.7

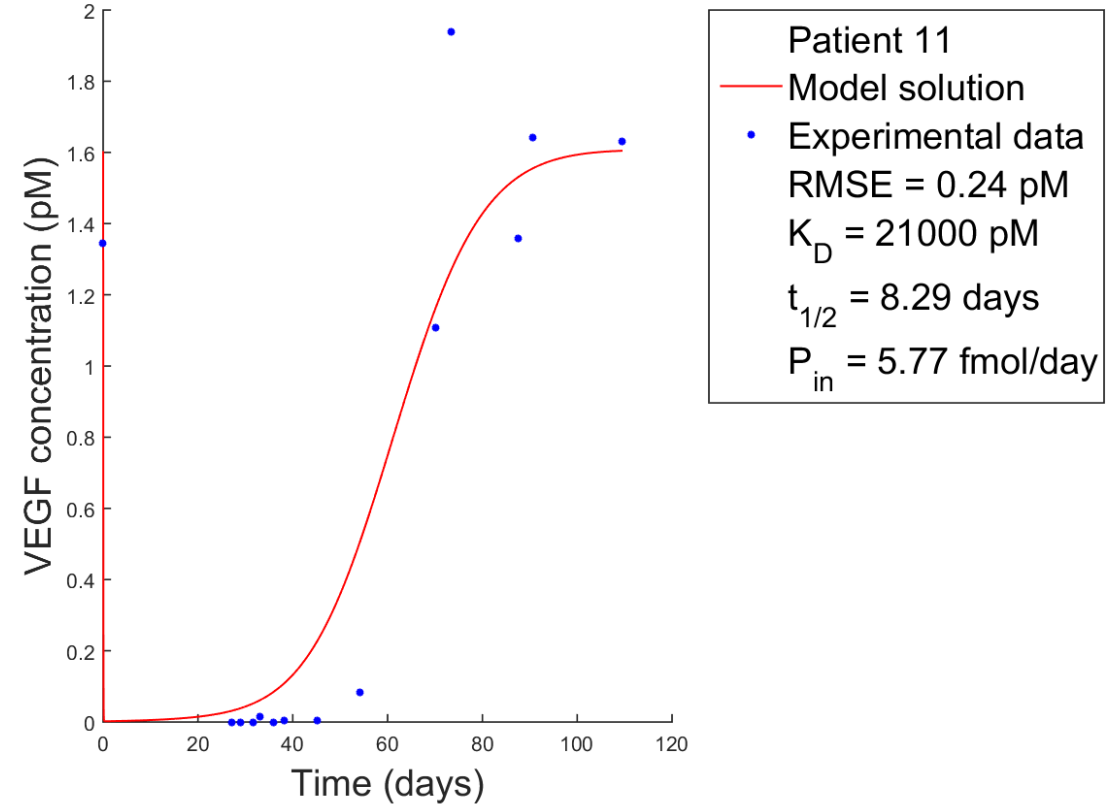
Patient 11
Model solution
Experimental data
RMSE = 0.24 pM
K_D = 21000 pM
t_1/2 = 8.29 days
P_in = 5.77 fmol/day
VEGF concentration (pM)
Time (days)
0
0.2
0.4
0.6
0.8
1
1.2
1.4
1.6
1.8
2
0
20
40
60
80
100
120

Figure S3.8

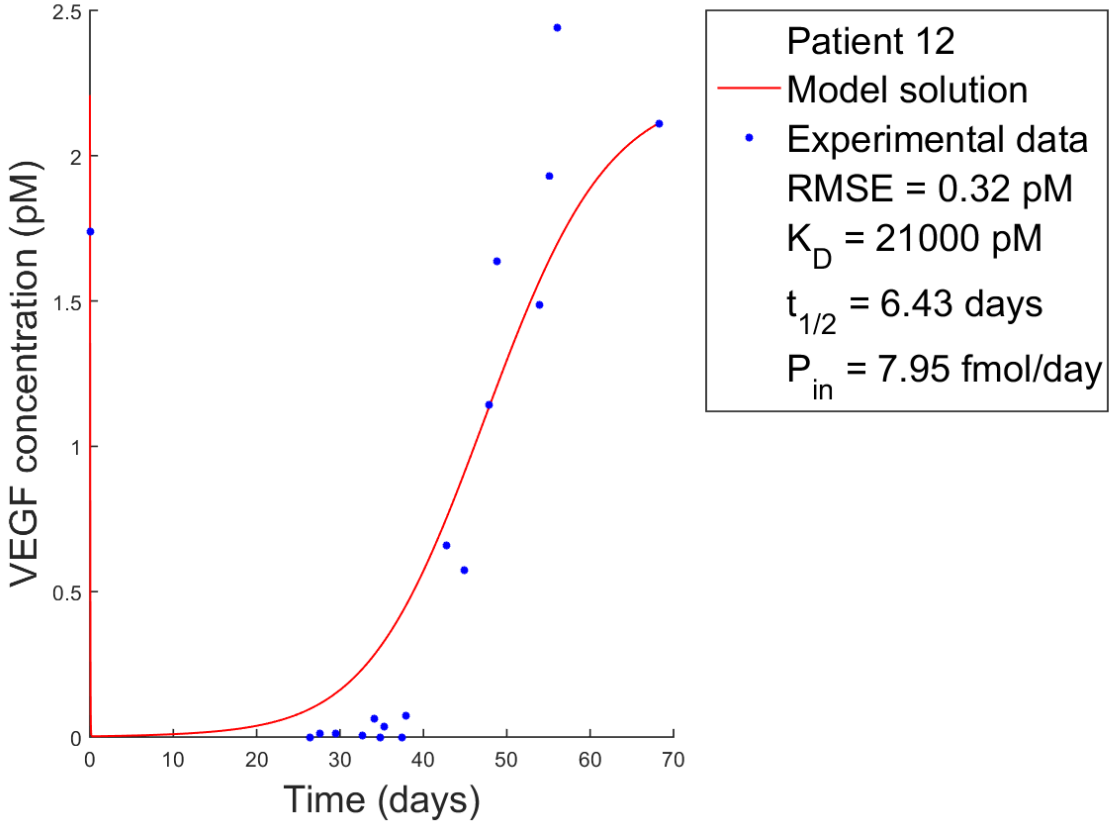
Patient 12
Model solution
Experimental data
RMSE = 0.32 pM
K_D = 21000 pM
t_1/2 = 6.43 days
P_in = 7.95 fmol/day
VEGF concentration (pM)
Time (days)
0
0.5
1
1.5
2
2.5
0
10
20
30
40
50
60
70

Figure S3.9

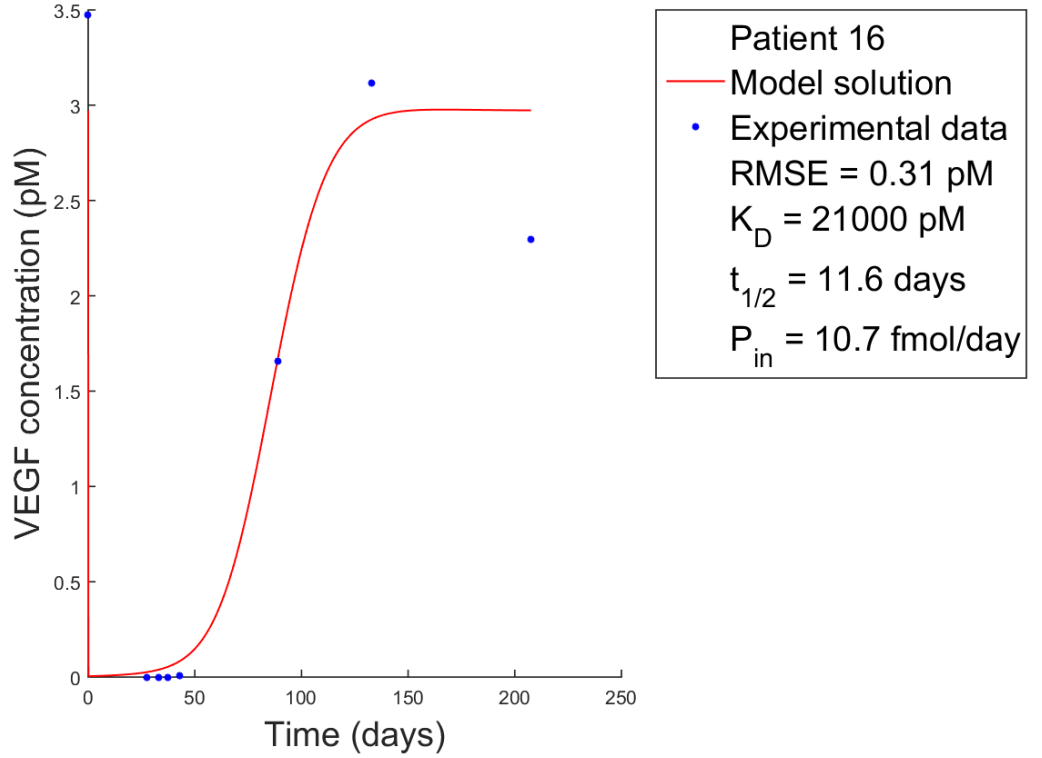

Figure S3.10

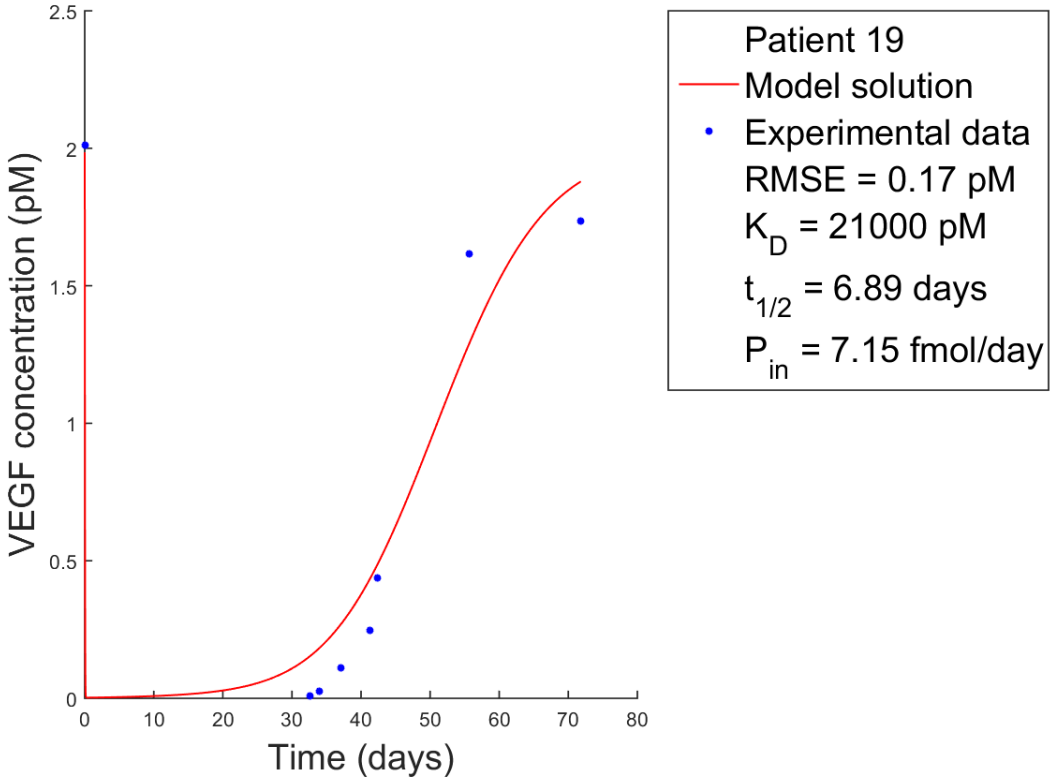

Figure S3.11

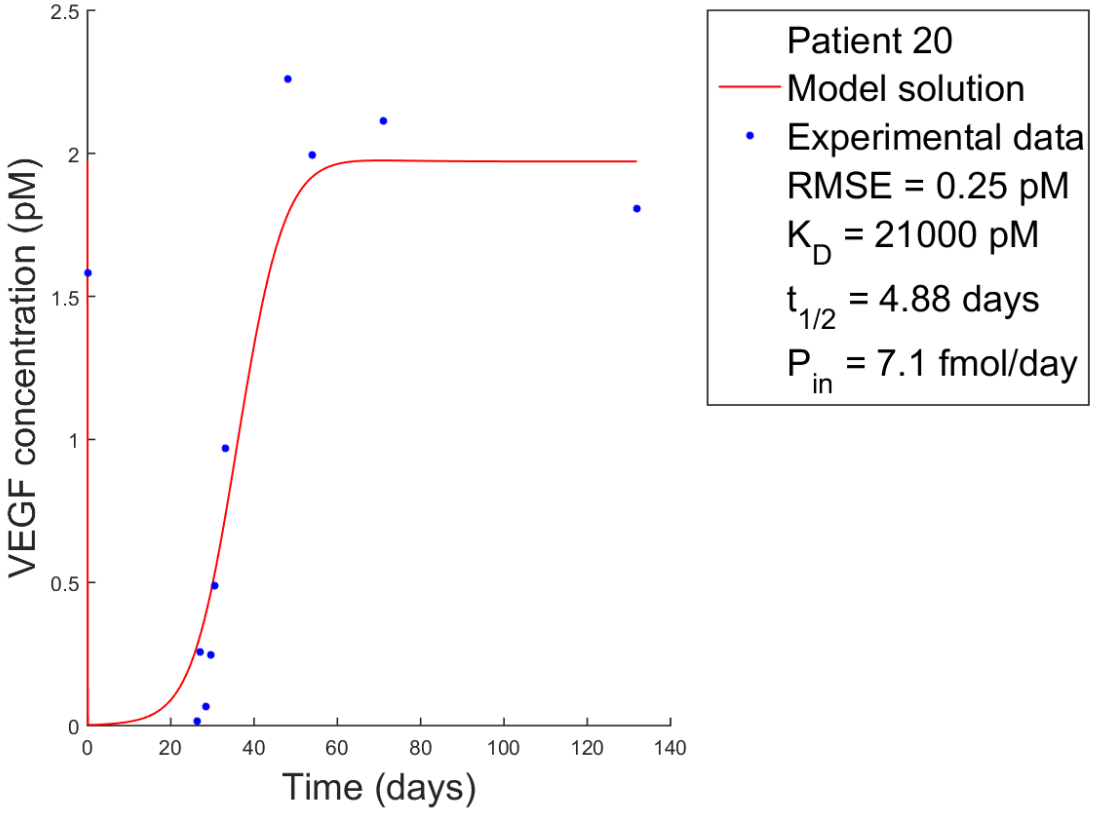

Figure S3.12

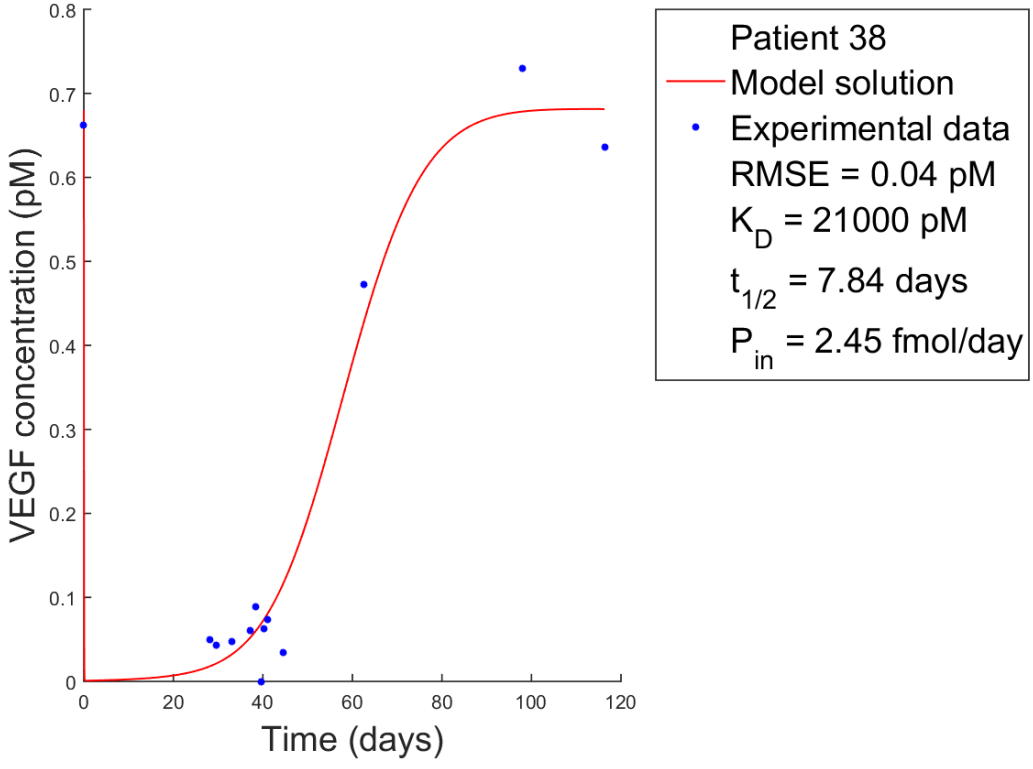

Figure S3.13

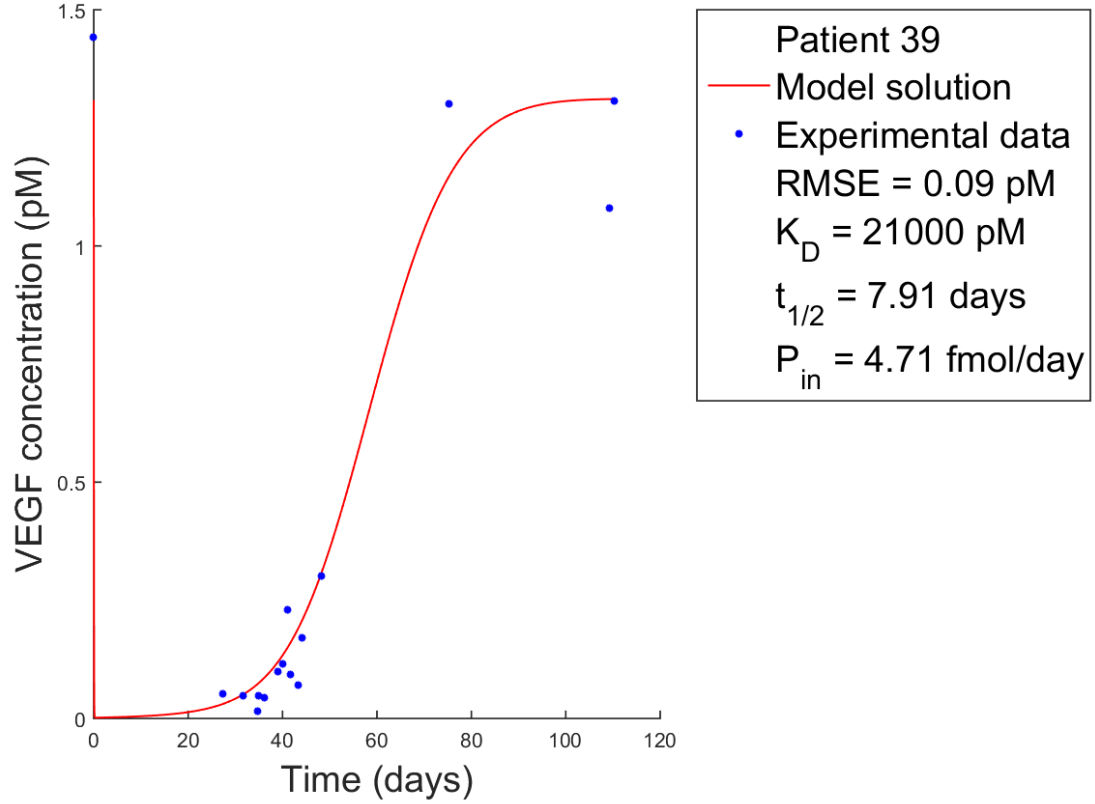

Figure S3.14

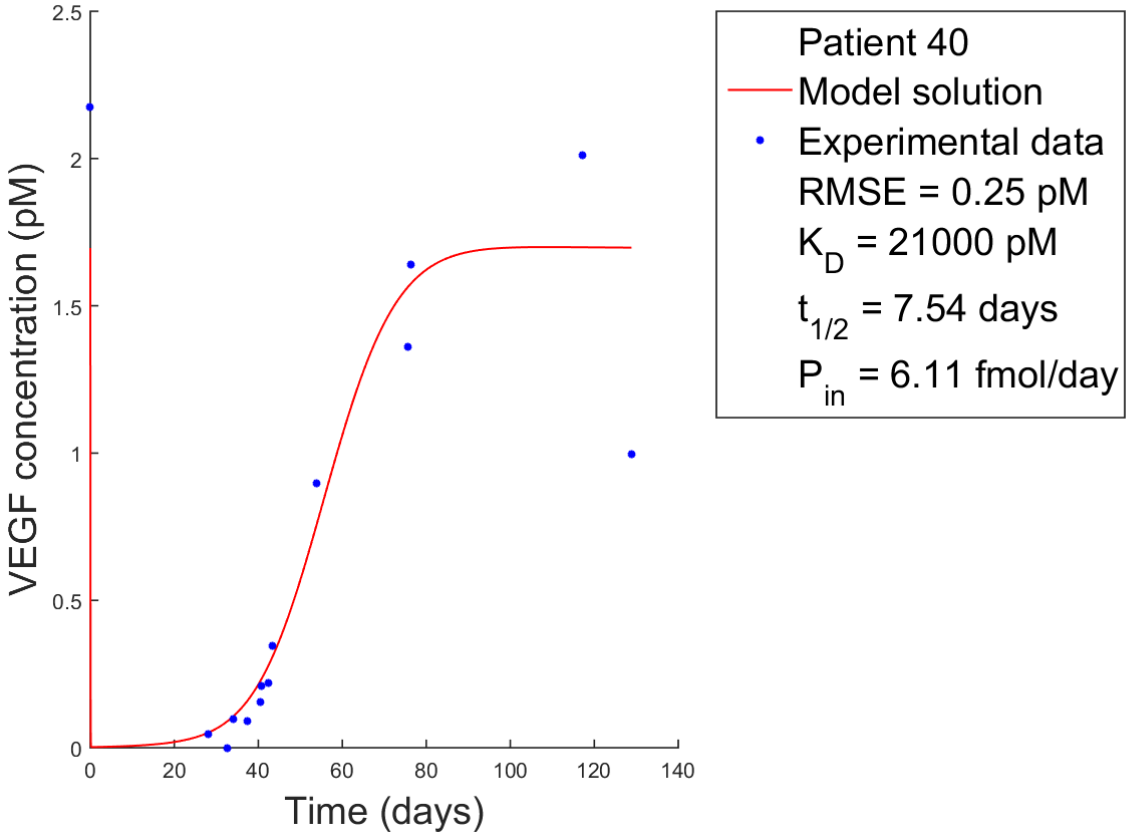

Figure S3.15

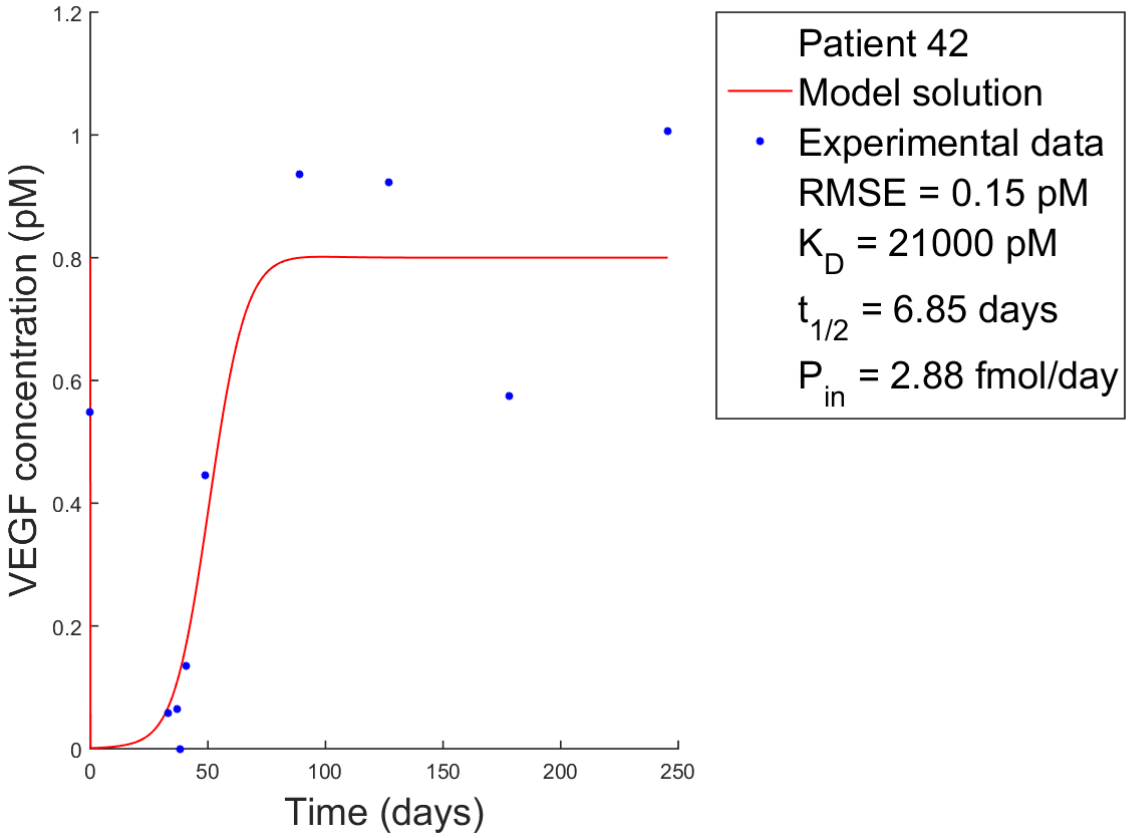

Figure S3.16

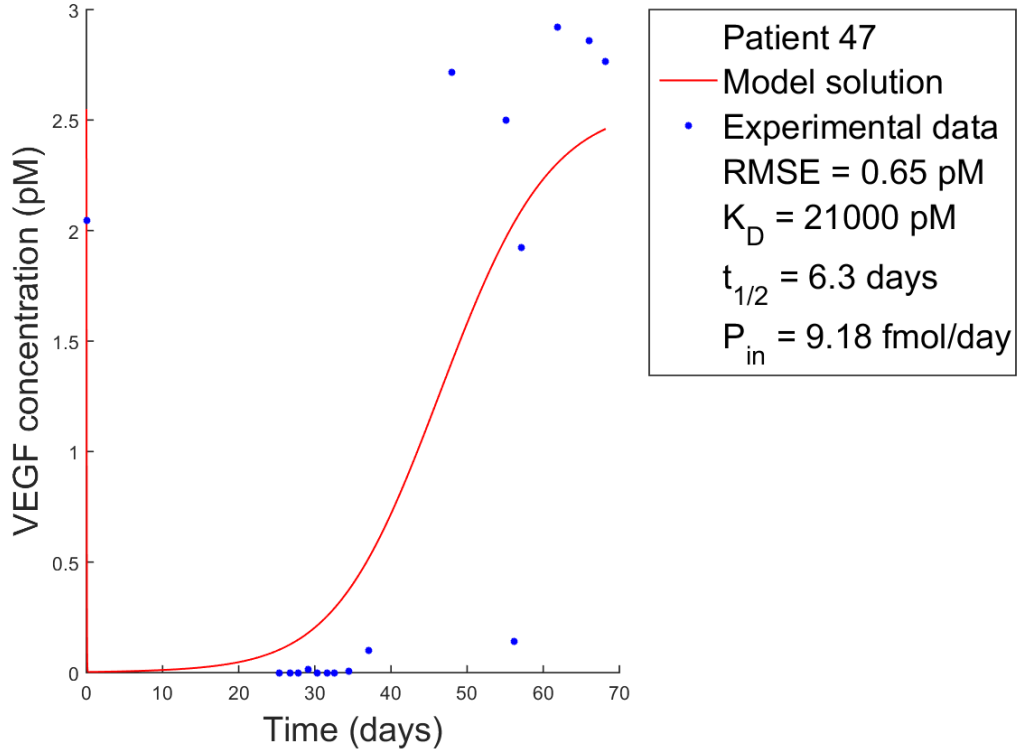

Figure S3.17

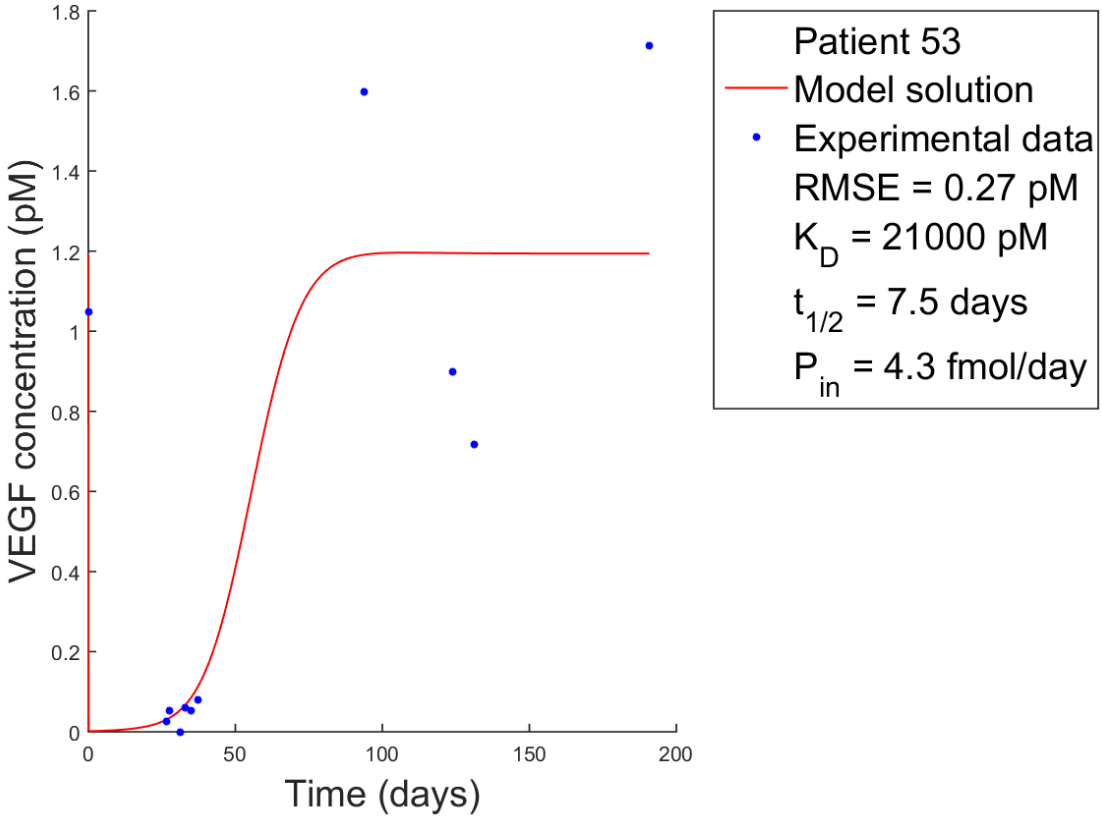

Figure S3.18

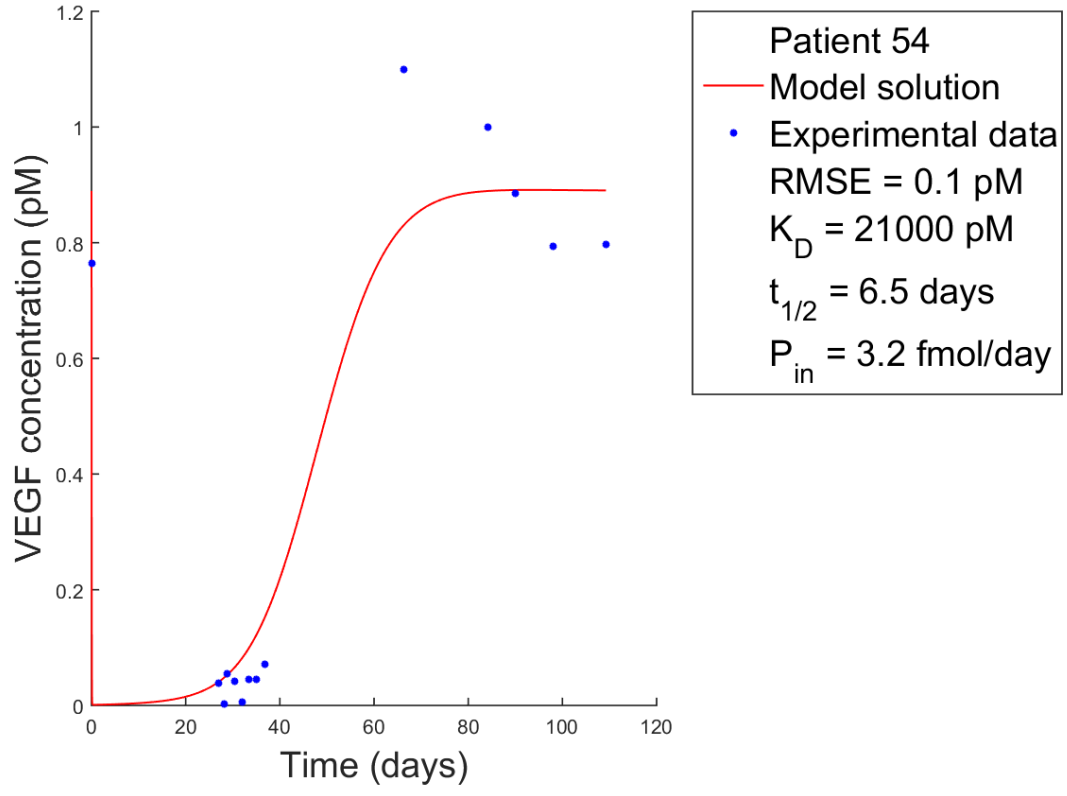

Figure S3.19

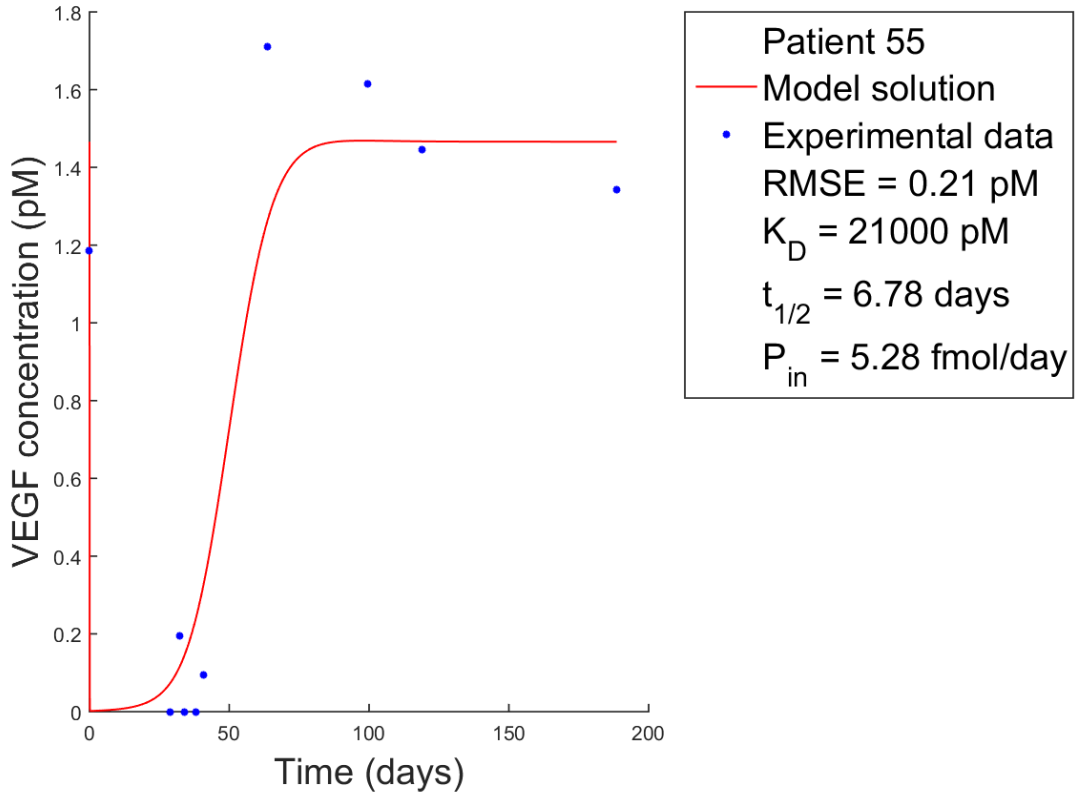

Figure S3.20

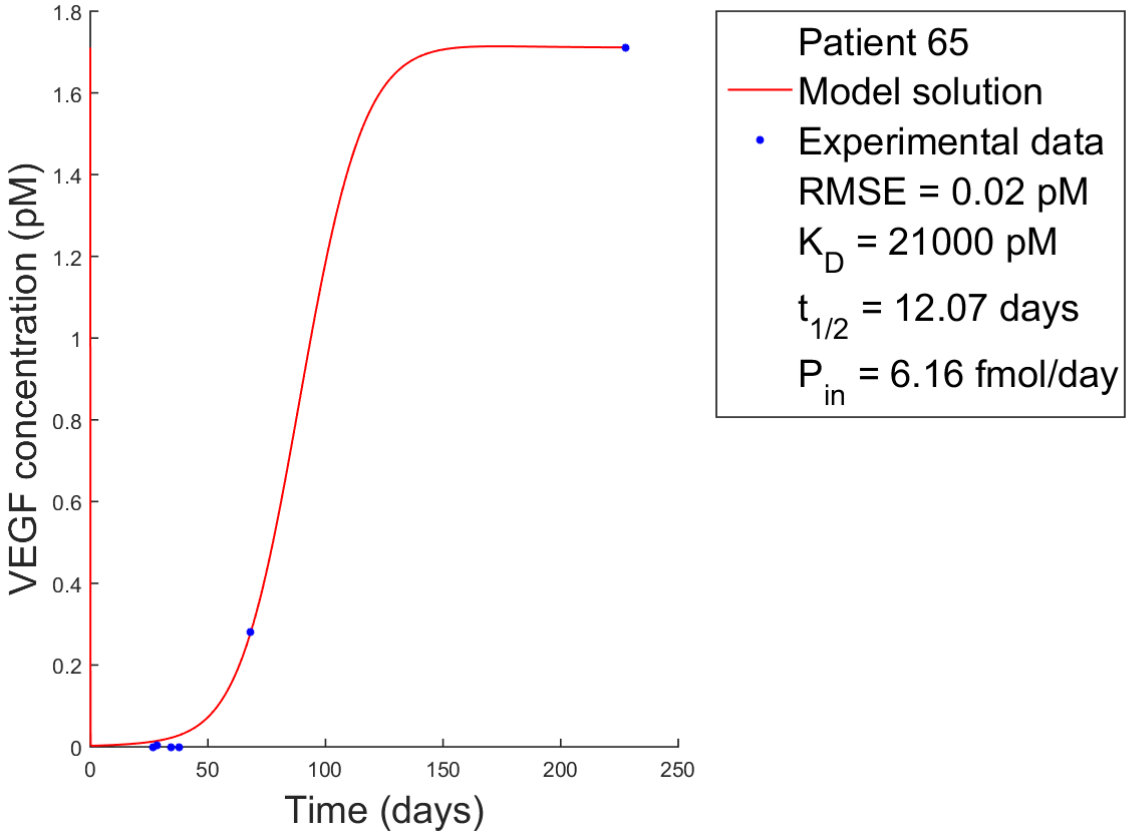

Figure S3.21

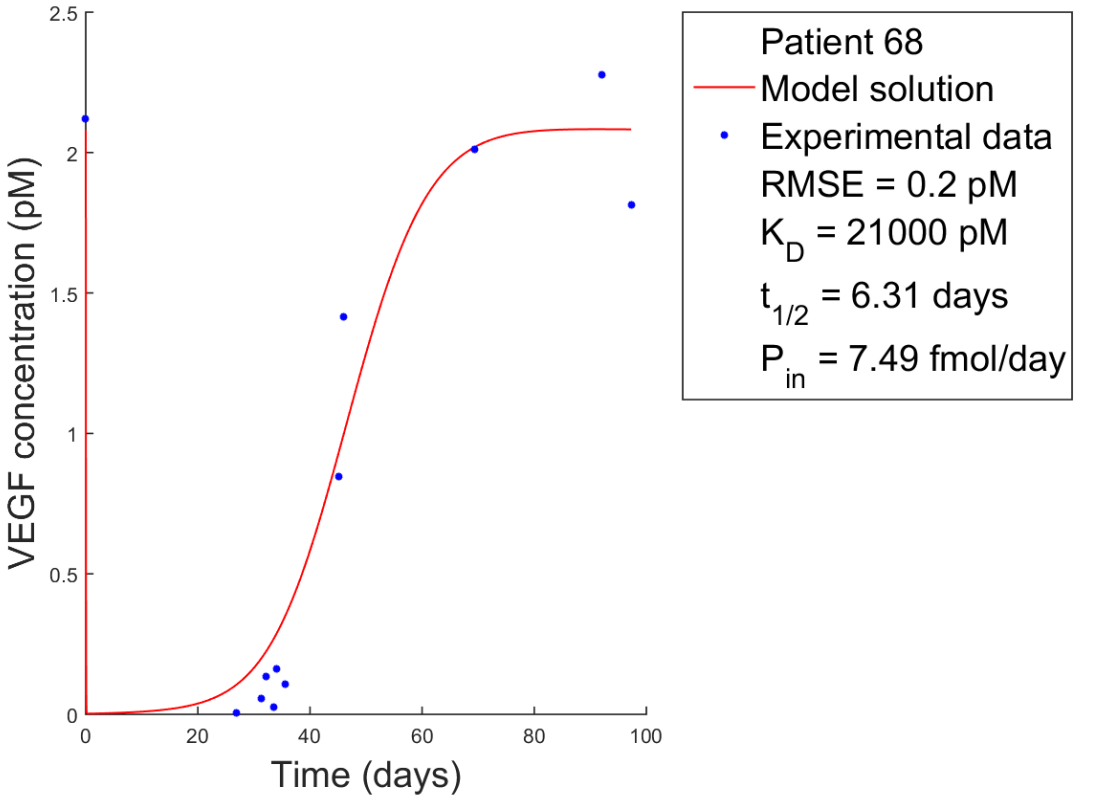

Figure S3.22

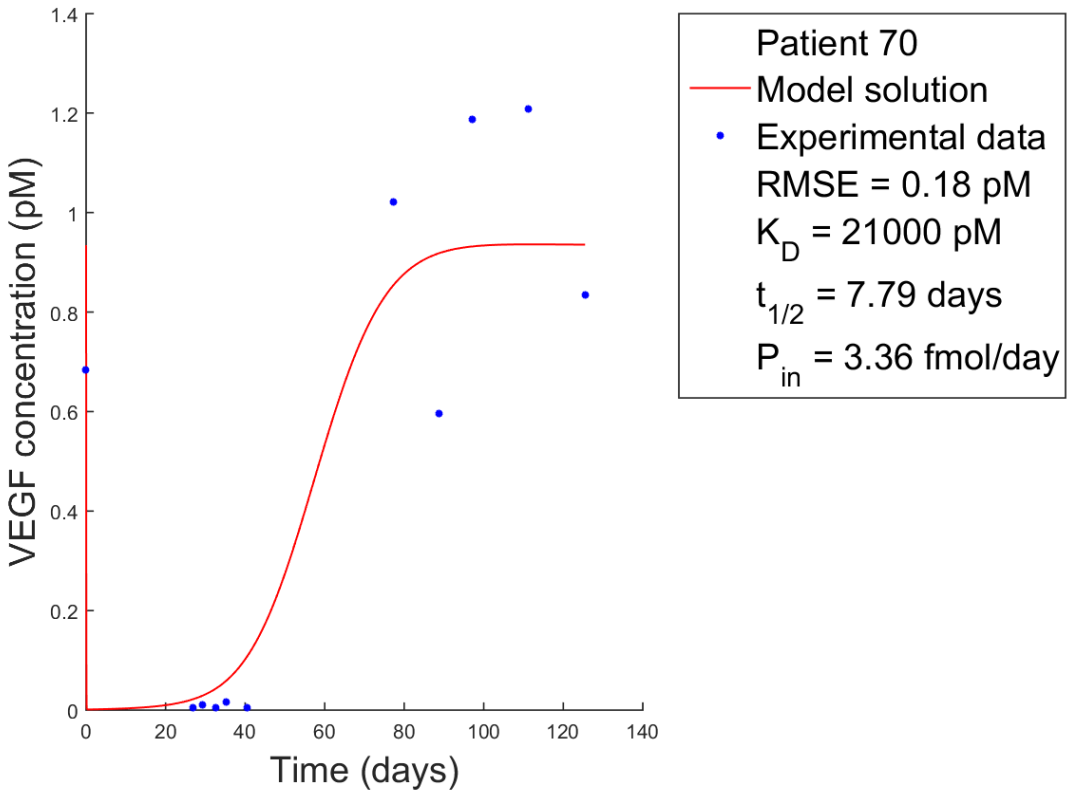

Figure S3.23

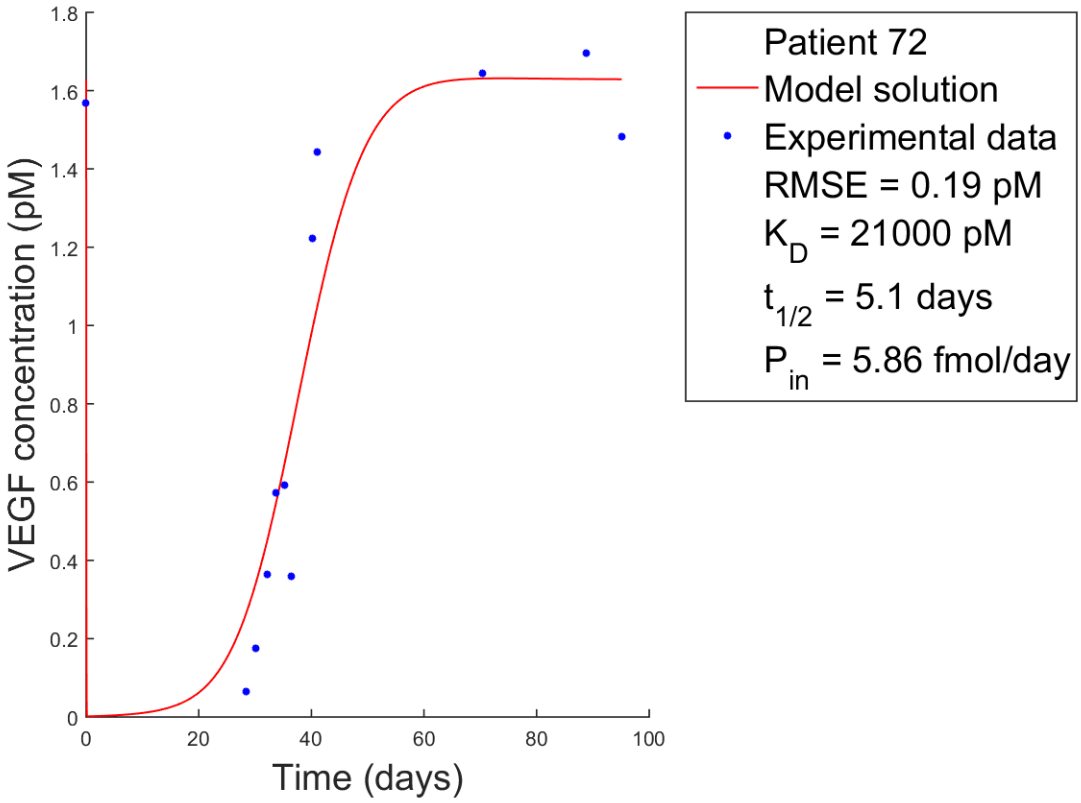

Figure S3.24

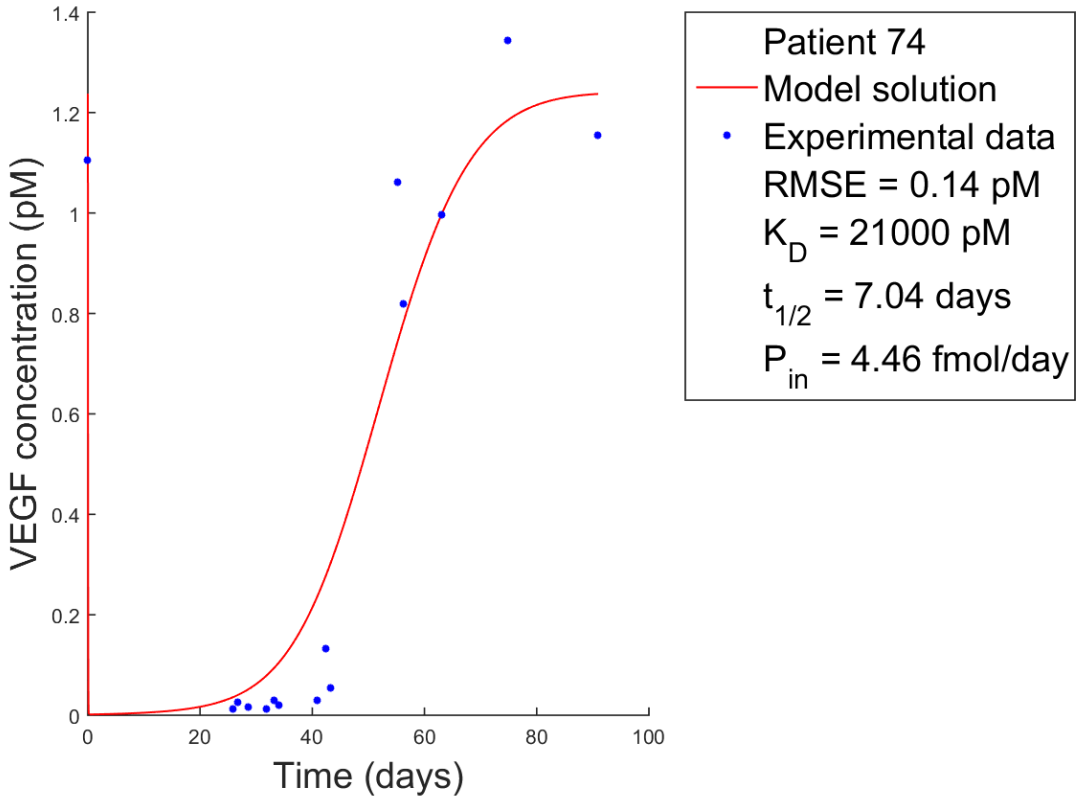

Figure S3.25

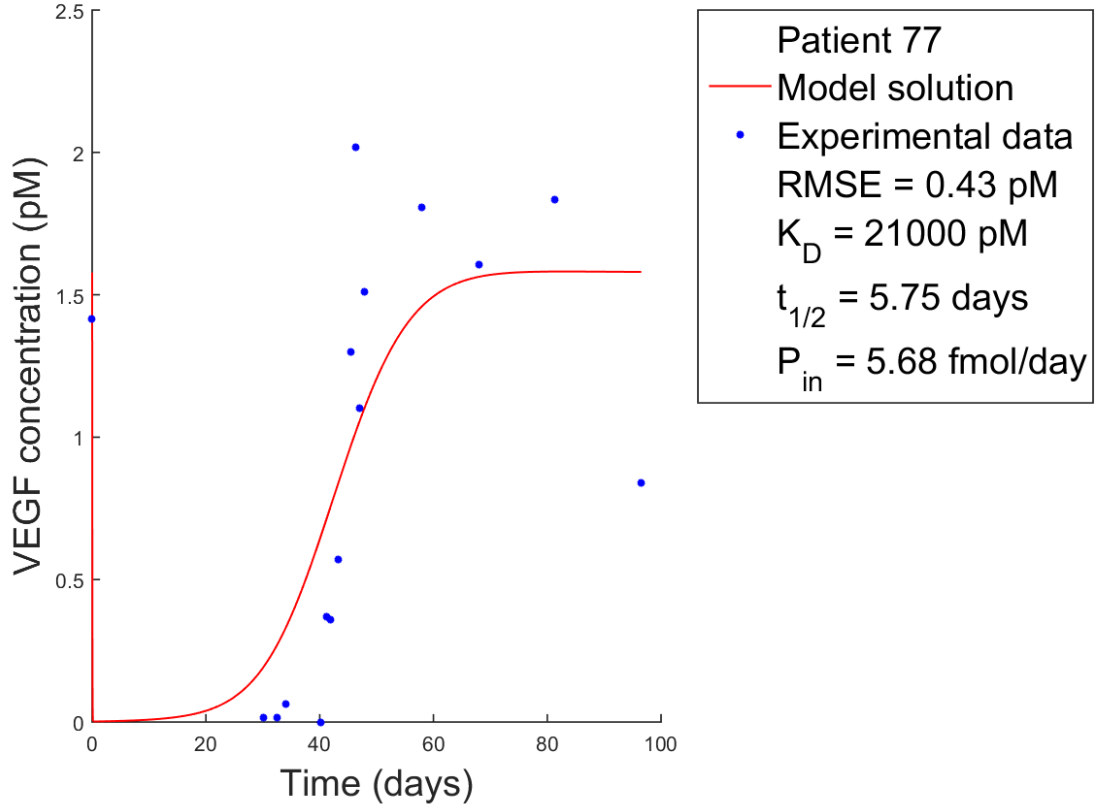

Figure S3.26

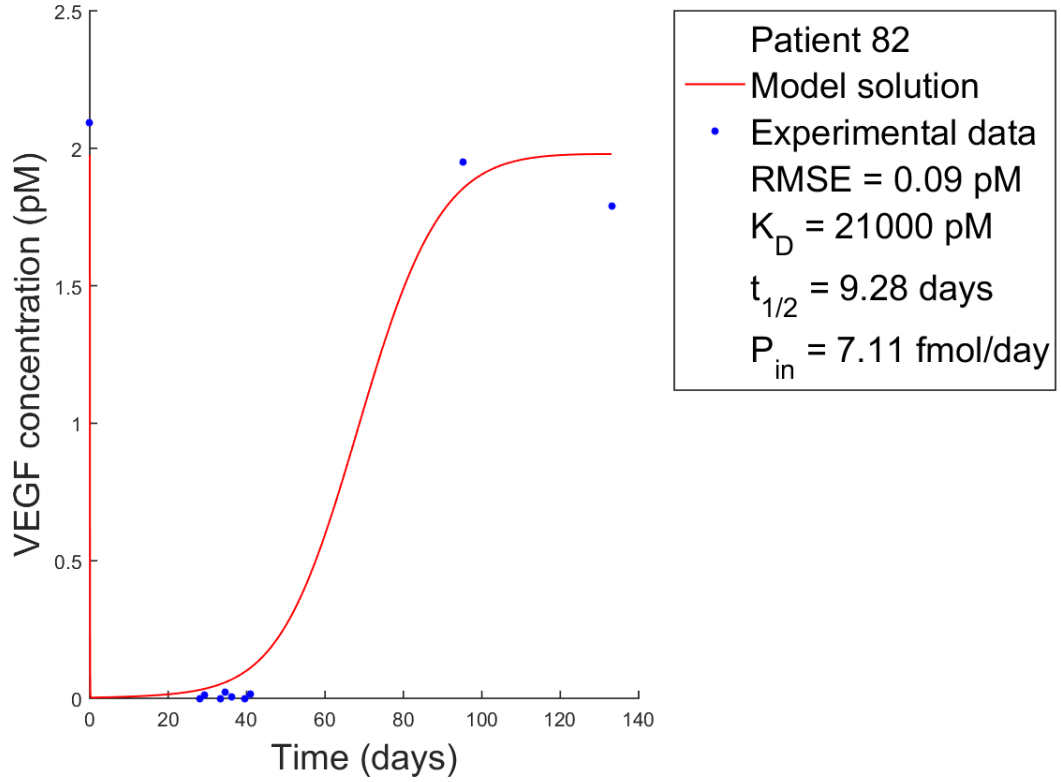

Figure S3.27

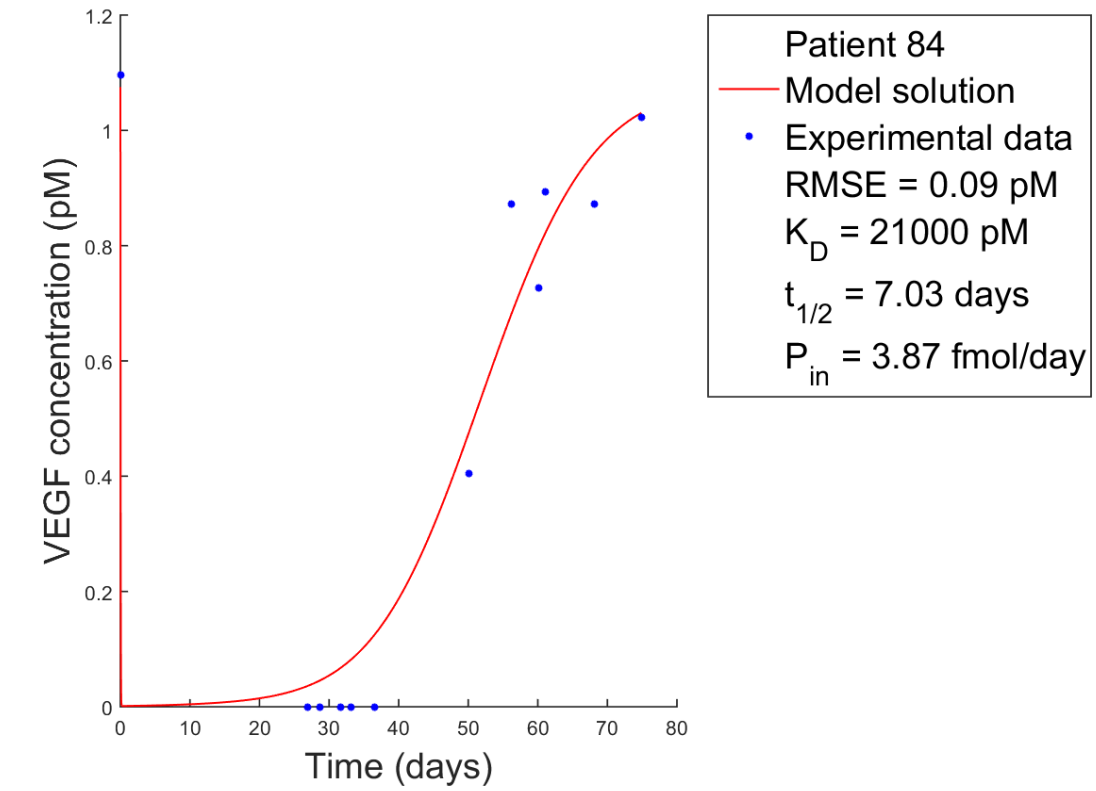

Figure S3.28

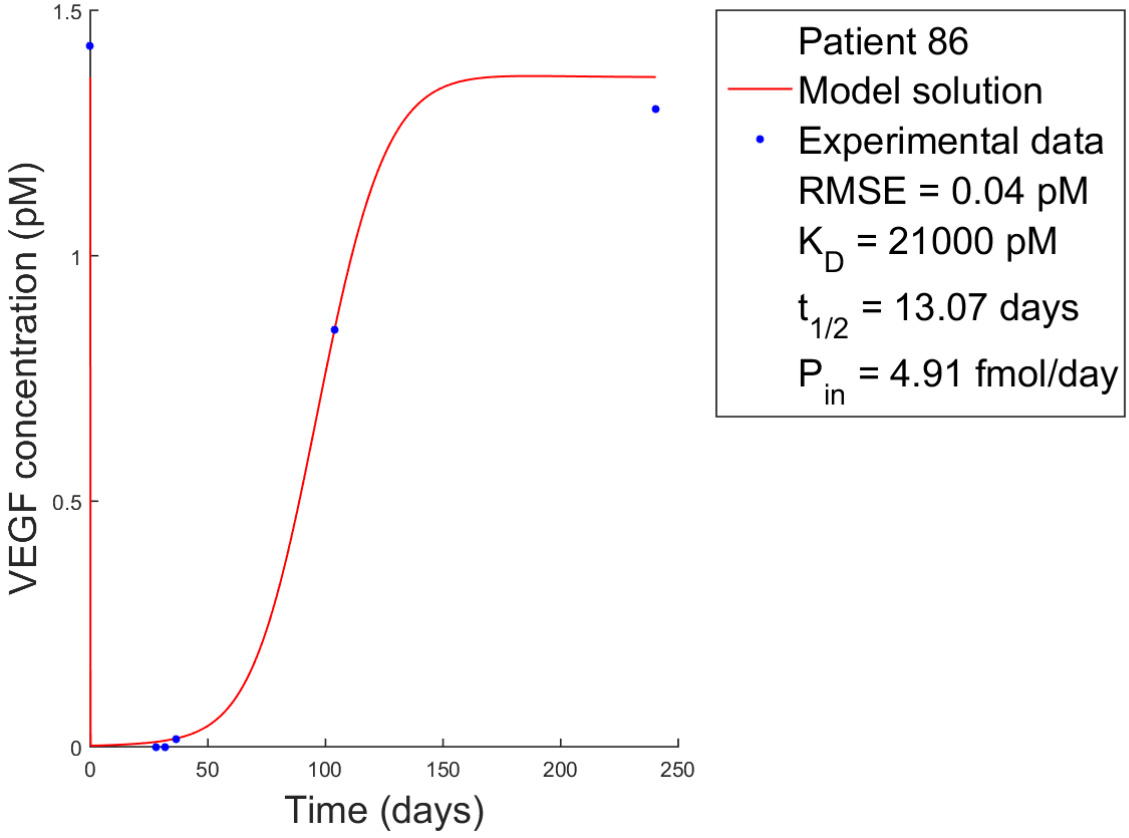

Figure S3.29

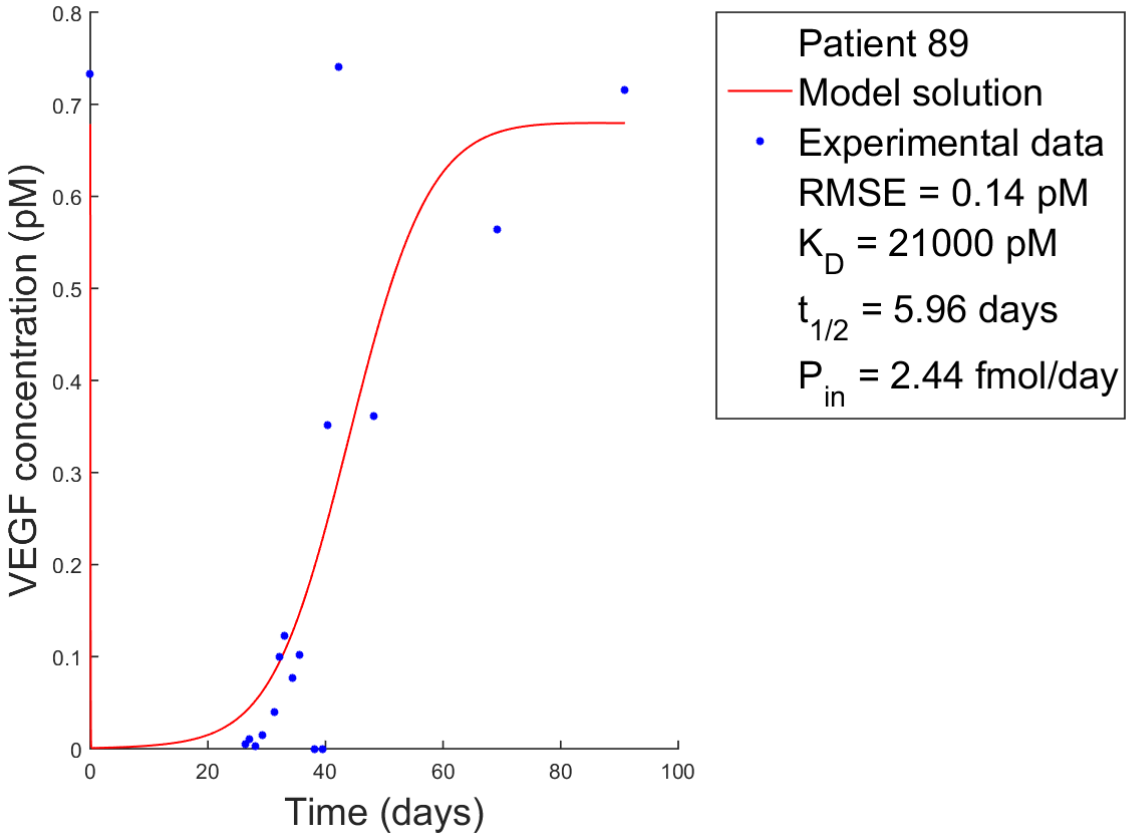
Patient 89
Model solution
Experimental data
RMSE = 0.14 pM
K_D = 21000 pM
t_1/2 = 5.96 days
P_in = 2.44 fmol/day
VEGF concentration (pM)
Time (days)
0
0.1
0.2
0.3
0.4
0.5
0.6
0.7
0.8
0
20
40
60
80
100

Figure S3.30

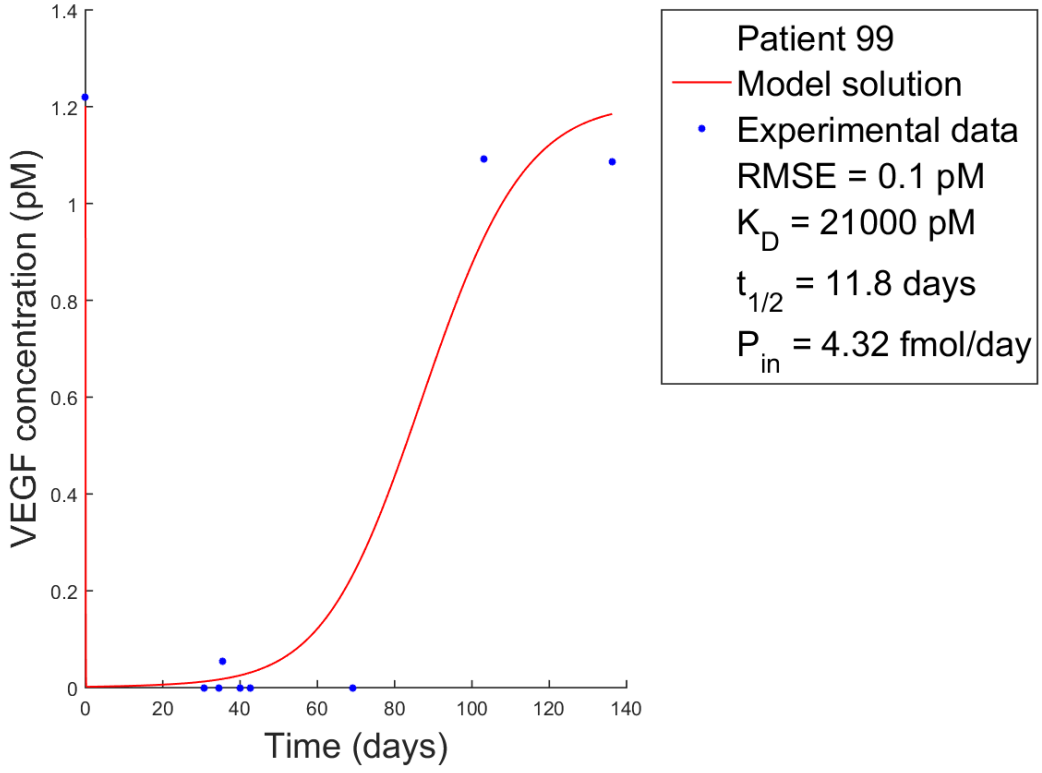
Patient 99
Model solution
Experimental data
RMSE = 0.1 pM
K_D = 21000 pM
t_1/2 = 11.8 days
P_in = 4.32 fmol/day
VEGF concentration (pM)
Time (days)
0
0.2
0.4
0.6
0.8
1
1.2
1.4
0
20
40
60
80
100
120
140

Figure S3.31

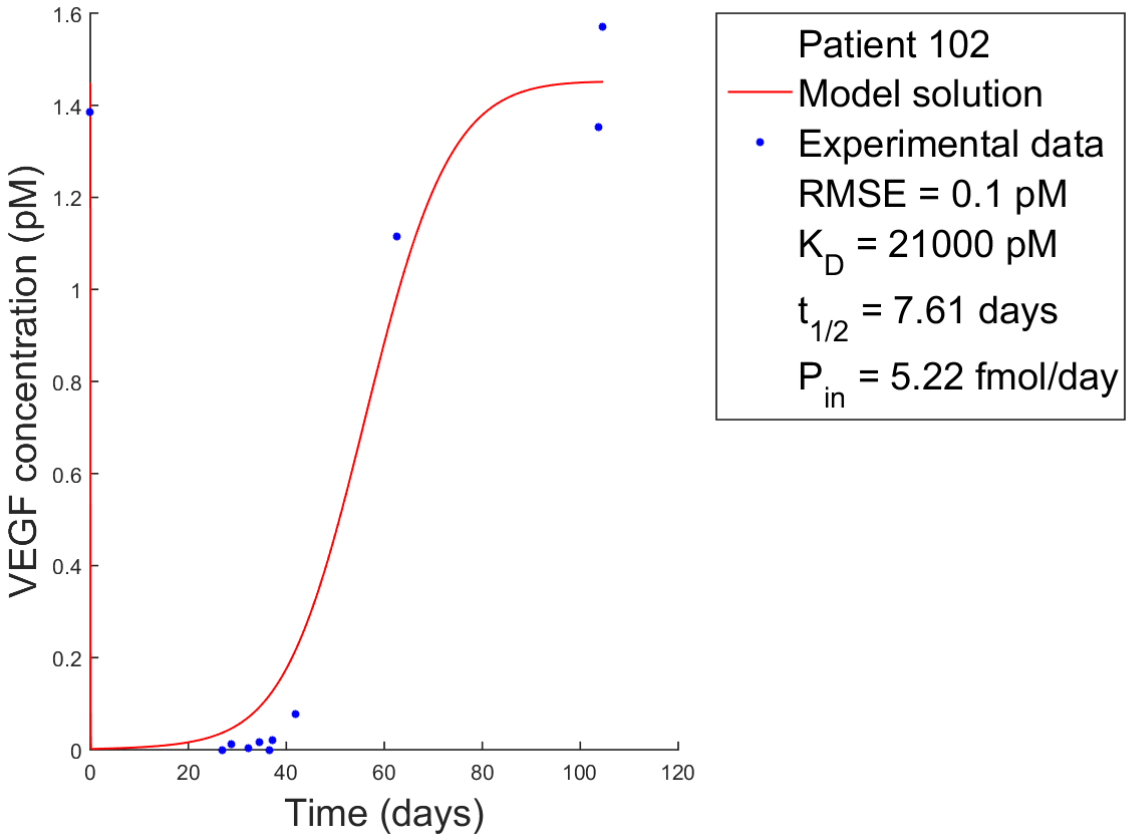
Patient 102
Model solution
Experimental data
RMSE = 0.1 pM
K_D = 21000 pM
t_1/2 = 7.61 days
P_in = 5.22 fmol/day
VEGF concentration (pM)
Time (days)
0
0.2
0.4
0.6
0.8
1
1.2
1.4
1.6
0
20
40
60
80
100
120

S4. RMSE plot for individual patients as a function of K_D

Figure S4.1: Dependence of root mean square error (RMSE) of optimized individual subject fits on K_D values over the range 50 to 60,000 pM. Numbers indicate patient IDs used by Sanders et al.[9] The weak increasing trends are not sufficient uniquely to determine the in vivo value of K_D from the data.

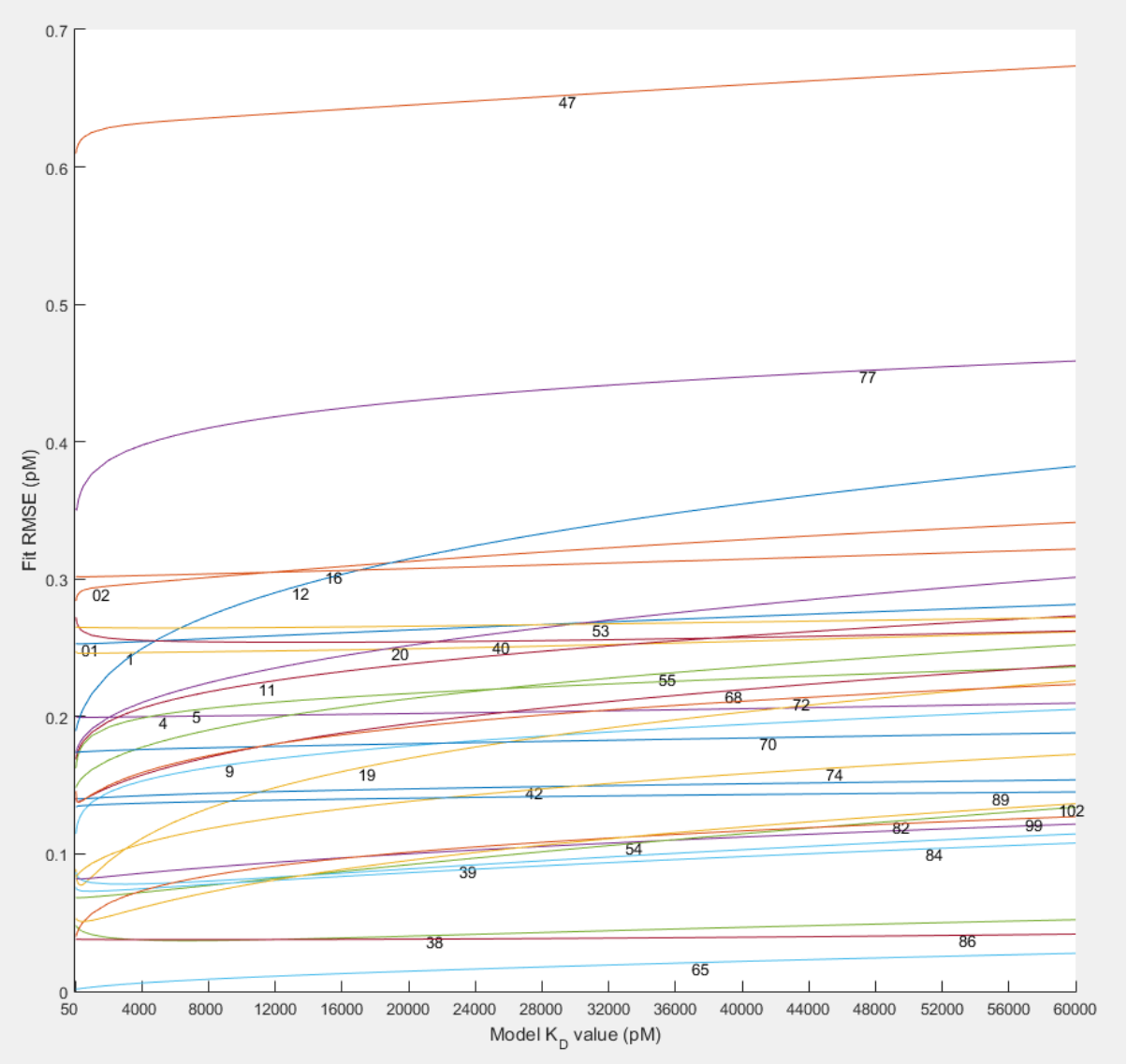

S5. Effect of k_{off} (days^{-1}) on VEGF profiles in the vitreous and aqueous chambers for K_D = 21,000 pM

Figure S5.1: Panels on left show the influence of increasing k_{off} on the profiles of V (red curve), VR (blue curve) and RVR (purple curve) in the vitreous chamber. Panels on the right show the corresponding profiles in the aqueous chamber. Dashed lines seen in the last three aqueous humor plots show the V, VR and RVR profiles from the previous plot (above) to indicate how the profile changes as k_{off} increases from k_{off} = 0.864 days^{-1} through to k_{off} = 864000 days^{-1}.

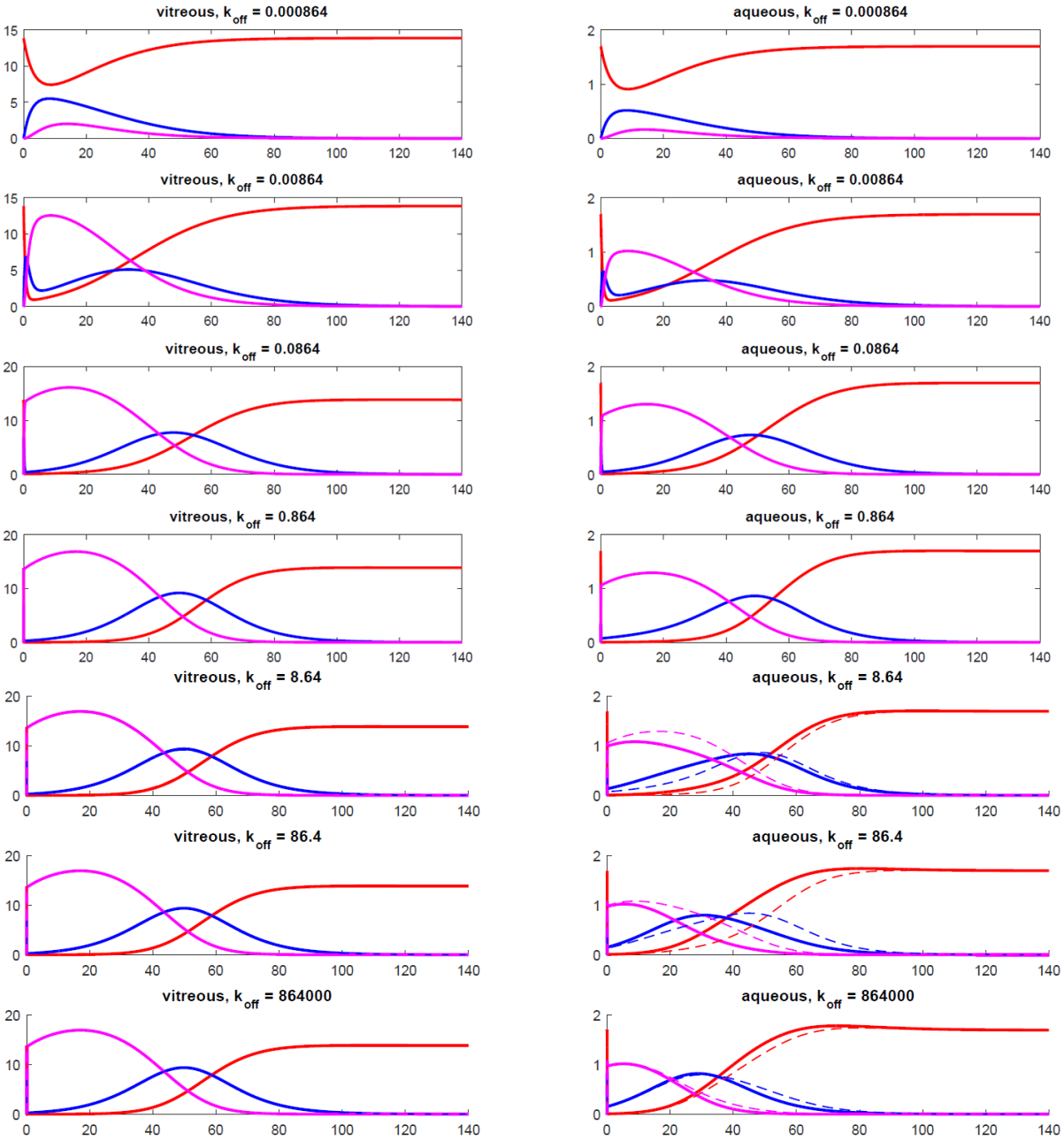

For k_{off} values of 0.864 day^{-1} and above the vitreous V profiles have already reached the quasi-equilibrium state, as k_{off} is much greater than the kel value for V (0.1 day^{-1}). In contrast ,the aqueous V profiles shift to the left until the quasi-equilibrium profile is attained due to the higher clearance

rate in the aqueous chamber, ca. 23 day^{-1} (CL_{aq}/Vol_{aq}). At low values of k_{off}, the V profiles do not reach the quasi-equilibrium state in either the vitreous or aqueous chambers.

S6. Theoretical dependence of VEGF suppression time on dose, KD and MW

Based on the RVR binding model for ranibizumab-VEGF interaction it can be shown that under quasi-equilibrium conditions (k_{off} >> kel) the time-dependence of the free VEGF fraction in the vitreous chamber, $FV_{vit}(t)$ will be given by:

Eq. S6.1 $$FV_{vit}(t) = 1/(1 + r_{vit}(t)/K_D)^2$$

where $r_{vit}(t)$ is the unbound vitreal concentration of R (or a new molecule that binds VEGF according to the RVR model) and K_D is the dissociation rate constant as defined previously. Neglecting the very small concentration of bound R in the vitreous chamber (which cannot exceed the total VEGF concentration of ca. 2 pM), $r_{vit}(t)$ (pM) will be given by:

Eq. S6.2 $$r_{vit}(t) = 10^{12}\, d_0/MW/Vol_{vit}\, \exp(-kel_R\, t)$$

where d_0 is the dose (mg), MW is the molecular weight (g/mole), Vol_{vit} is the vitreous volume (mL) and kel_R is the elimination rate constant of R.

Substitution of Eq. S6.2 into S6.1 yields:

Eq. S6.3 $$FV_{vit}(t) = 1/(1 + 10^{12}\, d_0/MW/Vol_{vit}\, \exp(-kel_R\, t)/K_D)^2$$

From this result and the relationship between kel_R and $t_{1/2R}$ (Equation (5)) we may derive the time (denoted TX%) where FV_{vit} has risen from a suppressed level to X%:

Eq. S6.4 $$TX\% = t_{1/2R}\, \ln(10^{12}\, d_0\, C_0(X)/MW/Vol_{vit}/K_D)/\ln(2)$$

where $C_0(X)$ is a dimensionless function given by:

Eq. S6.5 $$C_0(X) = 1/((100/X)^{1/2} - 1)$$

For a particular value of X%, e.g. 5% or 50%, Equations S6.4 and S6.5 give an explicit formula for the dependence of TX% on d_0 and K_D.

The effect of doubling d_0 is readily derived:

Eq. S6.6
$$\begin{aligned} TX\%(2d_0) - TX\%(d_0) &= t_{1/2R}\, \ln(10^{12}\, 2d_0\, C_0(X)/MW/Vol_{vit}/K_D)/\ln(2) \\ &\quad - t_{1/2R}\, \ln(10^{12}\, d_0\, C_0(X)/MW/Vol_{vit}/K_D)/\ln(2) \\ &= t_{1/2R}\, \ln(2)/\ln(2) \\ &= t_{1/2R} \end{aligned}$$

Thus regardless of the particular value of d_0, a doubling of the dose will shift the VEGF profile to the right by an amount equal to $t_{1/2R}$, a result also noted by Saunders[9]. This is illustrated in Figure S6.1 where the dose-dependence of T5% is shown for the full model simulation and the result of Equation S6.4 and S6.5 for X=5 (denoted theory).

Figure S6.1: Effect of dose on T5% based on full simulation and theory based on Equations S6.4 and S6.5. The particular value of $t_{1/2R}$ is 7.63 days and K_D is 22,000 pM.

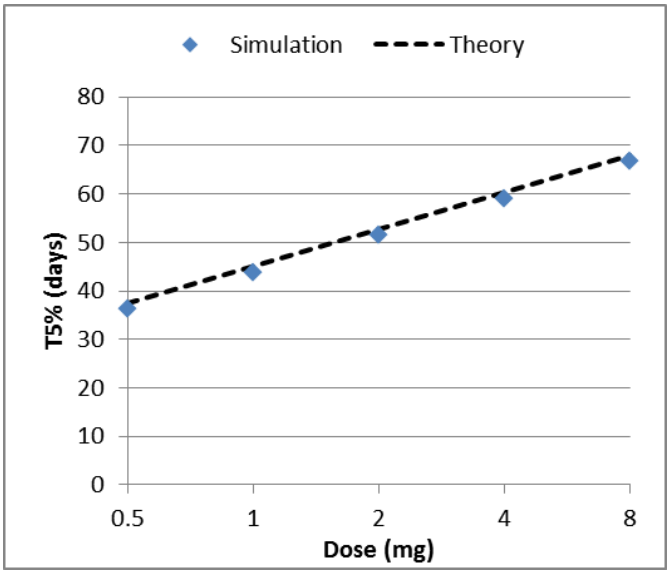

It can be similarly shown that for each 10-fold reduction of K_D, the TX% values will increase by:

Eq. S6.7 $$TX\%(K_D/10) - TX\%(K_D) = t_{1/2R} \ln(10^{12}\, d_0\, C_0(X)/MW/Vol_{vit}/(K_D/10))/\ln(2) - t_{1/2R} \ln(10^{12}\, d_0\, C_0(X)/MW/Vol_{vit}/K_D)/\ln(2)$$

$$= t_{1/2R} \ln(10)/\ln(2)$$

$$= 3.322\, t_{1/2R}$$

For $t_{1/2R}$ of 7.63 days, the increase is approximately 25 days, as shown in Figure S6.2 for T5%. As seen previously the theory is in close agreement with the full simulation.

Figure S6.2: Effect of K_D on T5% based on full simulation and theory based on Equations S6.4 and S6.5.

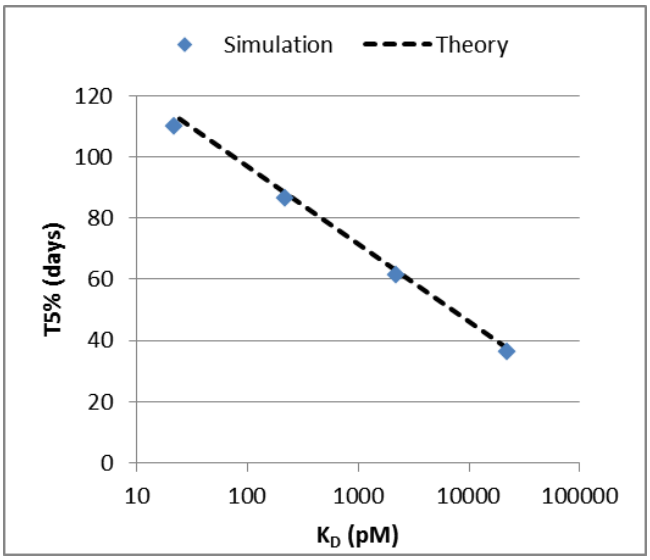

To simulate the effect of MW on TX%, we incorporate the effect of MW on $t_{1/2}$ into Equation S6.4, based on the scaling relationship of Equation (7):

Eq. S6.8 $TX\% = t_{1/2\,R0}\,(MW/MW_{R0})^{1/3}\,\ln(10^{12}\,d_0\,C_0(X)/MW/Vol_{vit}/K_D)/\ln(2)$

where $t_{1/2R0}$ is the half-life and MW_{R0} is the molecular weight of a reference species (R0), e.g., 7.63 days and 48,350 g/mole. Combining the fixed parameters into constants this result may be simply written as:

Eq. S6.9 $TX\% = C_1\,MW^{1/3}\,\ln(C_2(X)/MW)$

where: $C_1 = t_{1/2\,R0}\,/MW_{R0}{}^{1/3}/\ln(2)$ and $C_2(X) = 10^{12}\,d_0\,C_0(X)/Vol_{vit}/K_D$

We first consider the case where the administered dose d_0 is scaled to the MW, so that $C_2(X)/MW$ is constant. Under this condition TX% will increase with $MW^{1/3}$. This is illustrated for T5% in Figure S6.3 where MW is varied from 48,350 to 100,000, 200,000 and 500,000 g/mole with d_0 corresponding to 0.5, 1, 2 and 5 mg.

In the second case, d_0 is kept constant as the MW changes, which leads to a more complex dependence of TX% on MW. By differentiating Equation S6.9 with respect to MW, it can be shown that TX% will initially increase with MW up to a critical value MW* and decrease with MW thereafter. The critical value is given by:

Eq. S6.10 $MW^* = C_2(X)/e^3$

For T5% (X=5), d_0 = 0.5 mg, Vol_{vit} = 4.5 mL and K_D = 22000 pM, MW* will equal 72419 g/mole.

Figure S6.3 likewise shows the full simulation and theory corresponding to the fixed dose of 0.5 mg. The theory given by Equation S6.9 is in close agreement with the full simulation and as predicted by Equation S6.10, the maximum in T5% occurs between MW = 48,350 and 100,000 g/mole.

In all cases the analytical results, which are based on the quasi-steady state assumption in the vitreous chamber, provide excellent approximations to the full simulations and reflect the fact that the chosen value for k_{off} (0.864 day^{-1}) is large compared to the kel values.

Figure S6.3: Effect of MW on T5% based on full simulation and simplified theory for the cases of using a scaled dose (according to MW) and a constant dose of 0.5 mg.

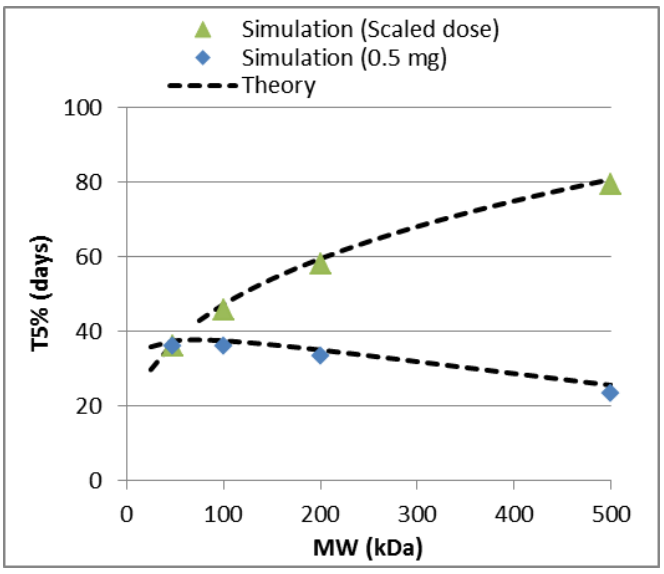

S7. References to the Supporting Information

(1) Missel, P. J. Simulating Intravitreal Injections in Anatomically Accurate Models for Rabbit, Monkey, and Human Eyes. *Pharm. Res.* **2012**, *29* (12), 3251–3272.

(2) Chuang, L.-H.; Wu, W.-C.; Yeung, L.; Wang, N.-K.; Hwang, Y.-S.; Chen, K.-J.; Kuo, J. Z.-C.; Lai, C.-C. Serum Concentration of Bevacizumab after Intravitreal Injection in Experimental Branch Retinal Vein Occlusion. *Ophthalmic Res.* **2011**, *45* (1), 31–35.

(3) Lin, Y. S.; Nguyen, C.; Mendoza, J. L.; Escandon, E.; Fei, D.; Meng, Y. G.; Modi, N. B. Preclinical Pharmacokinetics, Interspecies Scaling, and Tissue Distribution of a Humanized Monoclonal Antibody against Vascular Endothelial Growth Factor. *J. Pharmacol. Exp. Ther.* **1999**, *288* (1), 371–378.

(4) Gaudreault, J.; Fei, D.; Rusit, J.; Suboc, P.; Shiu, V. Preclinical Pharmacokinetics of Ranibizumab (rhuFabV2) after a Single Intravitreal Administration. *Investig. Ophthalmol. Vis. Sci.* **2005**, *46* (2), 726–733.

(5) Gadkar, K.; Pastuskovas, C. V.; Le Couter, J. E.; Elliott, J. M.; Zhang, J.; Lee, C. V.; Sanowar, S.; Fuh, G.; Kim, H. S.; Lombana, T. N.; Spiess, C.; Nakamura, M.; Hass, P.; Shatz, W.; Meng, Y. G.; Scheer, J. M. Design and Pharmacokinetic Characterization of Novel Antibody Formats for Ocular Therapeutics. *Investig. Opthalmology Vis. Sci.* **2015**, *56* (9), 5390–5400.

(6) Mordenti, J.; Cuthbertson, R. A.; Ferrara, N.; Thomsen, K.; Valverde, C. R.; Meng, Y. G.; David, T. W.; Fourre, K. M.; Ryan, A. M. Comparisons of the Intraocular Tissue Distribution , Pharmacokinetics , and Safety of 125 I-Labeled Full-Length and Fab Antibodies Following Intravitreal Administration. *Toxicol. Pathol.* **1999**, *27* (5), 536–544.

(7) Growth Chart for Sprague-Dawley rats, downloaded from http://www.criver.com/products-services/basic-research/find-a-model/sprague-dawley-rat, September 17, **2015**.

(8) Sha, O.; Kwong, W. H. Postnatal Developmental Changes of Vitreous and Lens Volumes in Sprague-Dawley Rats. *Neuroembryology Aging* **2006**, *4* (4), 183–188.

(9) Saunders, D. J.; Muether, P. S.; Fauser, S. A Model of the Ocular Pharmacokinetics Involved in the Therapy of Neovascular Age-Related Macular Degeneration with Ranibizumab. *Br. J. Ophthalmol.* **2015**, 1–6. doi:10.1136/bjophthalmol-2015-306771